University of Southern Queensland

Faculty of Health, Engineering & Sciences

Design and Development of a Fibre-Optic Microphone

A dissertation submitted by

Isaac Kennedy

in fulfilment of the requirements of

ENG4112 Research Project

towards the degree of

Bachelor of Engineering

Submitted: October, 2014

Abstract

Due mainly to the fact that fibre-optic sensors are typically more expensive than conventional electronic sensors, fibre-optic sensing remains a somewhat obscure field. Fibre-optic sensors do have significant advantages such as electromagnetic immunity and corrosion resistance, and find their place in applications where electronics cannot be used (Kersey 1996). The aim of this project is the design and construction of a fibre-optic microphone, the proposed application for which is photoacoustic spectroscopy.

The theory behind fibre-optics, fibre-optic sensors, and interferometry is explored to provide a background for the project. Examination of the concept of photoacoustic spectroscopy reveals how this application affects the requirements of the microphone. Specifically, the microphone must be able to lock to a specified frequency and respond with an amplitude proportional to the volume of an audio tone at this frequency.

Based on its relatively high sensitivity and the simplicity of construction from fibre-optic components, it is determined that the Mach-Zehnder is the best suited interferometer for the fibre-optic microphone. A design is proposed based on the Mach-Zehnder interferometer and is constructed using fibre-optic components. A lock-in amplifier's ability to lock to a specific frequency is well suited to the requirements of photoacoustic spectroscopy and is incorporated in the design as a means of extracting the microphone output.

Testing of the device produced promising results. The response of the fibre-optic microphone as measured by the lock-in amplifier is exponentially proportional to the volume of the tone used to test it. This proves the concept of the fibre-optic microphone and shows that it is fit for use in photoacoustic spectroscopy.

University of Southern Queensland

Faculty of Health, Engineering & Sciences

ENG4111/2 *Research Project*

Limitations of Use

The Council of the University of Southern Queensland, its Faculty of Health, Engineering & Sciences, and the staff of the University of Southern Queensland, do not accept any responsibility for the truth, accuracy or completeness of material contained within or associated with this dissertation.

Persons using all or any part of this material do so at their own risk, and not at the risk of the Council of the University of Southern Queensland, its Faculty of Health, Engineering & Sciences or the staff of the University of Southern Queensland.

This dissertation reports an educational exercise and has no purpose or validity beyond this exercise. The sole purpose of the course pair entitled "Research Project" is to contribute to the overall education within the student's chosen degree program. This document, the associated hardware, software, drawings, and other material set out in the associated appendices should not be used for any other purpose: if they are so used, it is entirely at the risk of the user.

Dean

Faculty of Health, Engineering & Sciences

Certification of Dissertation

I certify that the ideas, designs and experimental work, results, analyses and conclusions set out in this dissertation are entirely my own effort, except where otherwise indicated and acknowledged.
I further certify that the work is original and has not been previously submitted for assessment in any other course or institution, except where specifically stated.

Isaac Kennedy

0061016605

_____

Signature

_____

Date

Acknowledgments

This project was supervised by Dr. John Leis. I would like to thank him for his guidance, advice and support whilst completing the project.

I would also like to thank my friends and family for their support and patience throughout the course of the project, as well as the entire degree.

Isaac Kennedy

University of Southern Queensland
October 2014

Contents

List of Figures

List of Tables

Chapter 1

Introduction to the Design of a Fibre-Optic Microphone

Developments in low loss optical fibre and the laser in the 1960s led to increased research and use of fibre-optics for communications purposes. Following this in the 1970s a new field of research into fibre optic sensing emerged (Grattan & Sun 2000).

Fibre-optic sensors have several advantages over their conventional counterparts. This includes:

- Electromagnetic immunity
- Resistance to corrosion and aggressive chemicals
- High sensitivity
- Low loss

Fibre-optic sensors may also be designed to be compact and lightweight, and are suitable for remote sensing and multiplexing applications (Ecke, Chen & Jinsong 2012).

Previous research into fibre-optic microphones has been successful often having a better perceived response than conventional microphones (Kyriakou & Fisher 2013). Still, fibre-optic based microphones are not a common technology and few models are commercially available. Often fibre-optic sensors are employed in niche applications where

their unique properties are required. One example is the use of a fibre-optic microphone to record speech during Magnetic Resonance Imaging (MRI) scans. This would not be possible with a conventional microphone due to the strong magnetic fields employed in MRI (NessAiver, Stone, Parthasarathy, Kahana & Paritsky 2006).

1.1 Aim and Objectives

1.1.1 Aim

The aim of the project is to design and develop a fibre-optic microphone. The proposed application for the microphone is photoacoustic spectroscopy. Fibre-optic sensor theory provides many ways in which a fibre-optic microphone can be implemented, so an examination of current literature will be necessary in order to devise the most appropriate design for the application. Once a design has been conceived, it will be constructed and tested to evaluate its performance.

1.1.2 Objectives

The objectives of the project are as follows:

1. Research the theory behind the use of fibre-optic sensors in microphone and sound detection applications.
2. Investigate current work in the area of fibre-optic sensors, and fibre-optic microphones.
3. Based on the literature, devise the most appropriate design taking into account the application and available equipment.
4. Gather and study the use of the required equipment while preparing the necessary safety documentation.
5. Construct and test the fibre-optic microphone.

As time permits:

6. Investigate the use of a single-frequency lock-in configuration, and if possible test this concept.

7. Explore and discuss how the construction maybe improved including enhanced sensitivity, and reduced size and use of materials.

8. Implement and test any possible improvements discovered.

1.2 Methodology

The approach taken in completion of the project has a great impact on the outcome. Planning this approach before carrying out the project tasks can save time and improve overall outcome. This section outlines the methodology employed in completion of the project objectives.

1.2.1 Literature Review

A thorough literature review will be completed covering the theory relevant to the project, as well as similar work. The main resources used in research will be the USQ library and the USQ library website. It is important to scrutinise the source of information as this determines its accuracy and reliability. Textbooks and articles or research papers from reliable publications are a good sources of information and will be the major source of research for the project. Manuals put out by manufacturers will provide information on equipment where necessary.

The following are the major topics of the project and are important to the design of the fibre-optic microphone. These topics will form most of the background theory researched in the project.

Fibre-Optic Sensing

Fibre-optic sensing is of great relevance to this project. There are many ways in which a measurand can interact with the light guided inside the fibre and many of these can be used to detect sound. The project will require investigation of these methods. A

background on fibre-optic sensing is provided in Chapter 2.

Interferometry

The study of interferometry is closely linked to fibre-optic sensing. Interferometry offers great advantages to fibre-optic sensors, particularly those which rely upon phase modulation. As such, the concept of interferometry and the most relevant of the many existing interferometer configurations are also covered in Chapter 2.

Photoacoustic Spectroscopy

Photoacoustic spectroscopy is the proposed application for the fibre-optic microphone designed in this project. This application has significant impact on the requirements and design of the fibre-optic microphone. Photoacoustic spectroscopy will be covered in Chapter 3.

Lock-in Amplifiers

Lock-in amplifiers are used to find the amplitude of a signal at a known frequency despite a low Signal to Noise Ratio (SNR). Because the frequency used in photoacoustic spectroscopy can be controlled, lock-in amplifiers are of great advantage. Lock-in amplifiers are also covered in Chapter 3.

1.2.2 Testing

The fibre-optic microphone will undergo extensive testing in order to evaluate its performance. A test will be performed to investigate each parameter of interest. A description of each test will be given as well as the experiment setup used.

The method for each test will be made clear in a step-by-step procedure. This will enable the experiment to be repeated if necessary.

Recorded numerical results will be given in a table, and where appropriate, the data will be plot. In many cases, curve fitting will be appropriate. The trend of the data

must be identified and the least squares method will be employed to find the coefficients of the curve that fit the data.

1.2.3 Analysis of results

The results will be discussed after each test. Any observations or conclusions that can be gained from the results will be presented in this discussion.

1.3 Resources

All resources used in the project are provided by USQ. Care has been taken in selecting and using components, such that they can be used in future projects. In this way, very little waste is produced.

The following lists the equipment used to construct the microphone itself:

Optical Source: Thorlabs S1FC 1550nm Bench Top Laser

Photodetector: Thorlabs PGA8GS Photodetector

Couplers: Thorlabs 102020A 2x2 50:50 Couplers

Lock-in Amplifier: Ametek Signal Recovery Model 7270

These items are covered in further detail in Chapter 4. The following are additional items which are used in testing the device:

Function Generator: RIGOL DG4062 Function/Arbitrary Waveform Generator

Sound Level Meter: Larson Davis SoundTrack LxT1

More information on testing equipment is given in Chapter 5.

1.4 Timeline

Time management is vitally important to the success of the project. In order to ensure that tasks are completed on time, a timeline has been created. A Gantt chart was chosen to construct the timeline as it shows visually how tasks are managed simultaneously, and when they must be completed to meet deadlines. The timeline Gantt chart is shown in Appendix D.

1.5 Safety

Health and safety is the first priority in any engineering project. As such, a risk management plan has been prepared and included as Appendix B. The precautions therein are to be adhered to throughout the project.

1.6 Overview of the Dissertation

This dissertation is organised as follows:

Chapter 2 covers the basic concepts of fibre-optics and fibre-optic sensors.

Chapter 3 introduces photoacoustic spectroscopy and discusses why interferometry and lock-in amplifiers are well suited to this application.

Chapter 4 proposes a fibre-optic microphone design.

Chapter 5 evaluates the performance of the fibre-optic microphone. To this purpose, a number of tests are performed. The set up, procedure and results of each test are shown an discussed in this chapter.

Chapter 6 is the conclusion of the dissertation. This section reviews the major achievements of the project and discusses further work in the area.

Chapter 2

Fibre Optics and Fibre Optic Sensors

This chapter covers the theory of fibre-optics and fibre-optic sensors. The construction of optical fibre and the way in which it is possible to guide will be discussed in this chapter. The means by which a measurand can interact with fibre-optic components to form fibre-optic sensors will be addressed.

2.1 Refraction

It is known that the speed of light in free space is close to 3×10^8 m/s (Baird 1967). However, in any given medium, the propagation velocity u of light or any electromagnetic wave will be less than this according to the permeability and permittivity of the medium:

$$u = \frac{1}{\sqrt{\mu\epsilon}} \tag{2.1}$$

(Sadiku 2010, p. 459)

In this equation, permeability μ is the product of the medium's relative permeability and the permeability of free space ($\mu_0\mu_r$) and permittivity ϵ is the product of the medium's relative permittivity and the permittivity of free space ($\epsilon_0\epsilon_r$).

This leads to the refractive index n of the medium which is the ratio of the speed of light in free space c, to the speed of light in the medium (propagation velocity u):

$$n = \frac{c}{u} = c\sqrt{\mu\epsilon} \tag{2.2}$$

(Sadiku 2010, p. 487)

Refraction occurs when a ray of light passes through the boundary of two media with dissimilar refractive indices. As the wavefront approaches the boundary at an angle, it does not cross instantaneously. Instead there is an instance where the wavefront exists partially on either side of the boundary. As the two media have different propagation velocities, part of the wave front is travelling at a different velocity at this instant. This causes the ray to change direction. The exception is when the ray approaches from the normal (completely perpendicular to the boundary), in which case it continues along the normal upon crossing the boundary. The angle between the approaching ray of light and the normal is called the angle of incidence θ_i and the angle between the refracted ray and the normal is called the angle of refraction θ_r. The change in velocity which occurs at the boundary of the two materials will also cause a change in frequency (Crisp 1996).

2.2 Total Internal Reflection

Snells law defines the relationship between angles involved in the refraction of light at the border of two materials. Snell's law states:

$$n_i \sin\theta_i = n_r \sin\theta_r \tag{2.3}$$

(Crisp 1996)

Where n_i is the refractive index of the media where the ray originates, and n_r is the refractive index of the media into which the ray is refracting. Snell's law shows how the angle of refraction depends upon the angle of incidence and the refractive indices of the two materials:

$$\theta_r = \arcsin\left(\frac{n_i}{n_r}\sin\theta_i\right) \tag{2.4}$$

As the angle of incidence is increased, there will be a point where the angle of refraction is 90°. This means that the ray of light is refracted along the boundary of the two materials. The angle of incidence required to produce this effect is known as the critical angle θ_c. Remembering $\sin 90° = 1$, the critical angle can be calculated by modifying Snell's law:

$$\theta_c = \arcsin\left(\frac{n_r}{n_i}\right) \tag{2.5}$$

If an angle of incidence equal to the critical angle causes the refracted ray to travel along the boundary, then increasing the angle of incidence beyond this point will cause the refracted ray to reflect back into the first medium. This is known as Total Internal Reflection (TIR) and is the effect that makes light guiding possible. If two of the boundaries discussed here are in parallel, then the angle of incidence of a ray of light which is refracted internally will be repeated on the opposite side. This causes a repeated instance of TIR and the light continues at constant angle confined between the two boundaries. It should be noted that in order for total internal reflection to occur, the material that the ray of light is directed into must have a higher refractive index then the original medium to achieve total internal reflection. This is seen in (2.5), as a solution for critical angle is only possible when $\frac{n_r}{n_i}$ is greater than one (Crisp 1996).

2.3 Fibre Construction

The construction of optical fibre is based on the principal of TIR. It is possible to guide light in a fibre (usually constructed of glass or plastic) surrounded by a medium of higher refractive index. The surrounding medium could theoretically be as simple as air if the fibre has a refractive index lower then air. However, this would introduce many problems as the refractive index of the external medium would be unpredictable due to dirt and grease which would inevitably be introduced, as well as consideration of the material the fibre is resting on. Hence it is much more practical to surround the fibre in a coating of glass or plastic with a higher refractive index. This coating is called the cladding (Crisp 1996).

Glass is naturally flexible, but microscopic imperfections which form in the manufac-

turing and handling of the glass result in the glass shattering upon being bent. To counteract this, a plastic coating, referred to as the primary buffer, is applied. This prevents microscopic imperfection in the core and cladding, allowing the fibre to be flexible. A typical buffer may have a diameter of $250\mu m$. Further protective layers are usually added to the final product and are referred to as the jacket (Crisp 1996).

2.4 Numerical Aperture

A light ray travelling through an optical fibre strikes sides of the fibre with an angle of incidence which is greater than or equal to the critical angle as shown previously. It follows then that the angle of the light exiting the end of the fibre will also be greater than or equal to the critical angle. As the light exits the end of the fibre it refracts into the air, or other material at the end of the fibre. The normal at this boundary is in line with the fibre itself. This is perpendicular to the boundary between the core and the cladding of the fibre, so the maximum angle of incidence as the light exits the end of the fibre is $90° - \theta_c$. If the refractive indices of the core n_{core} and the external medium n_{external} are known, the angle of the light escaping the end of the fibre θ_{out} can then be found by Snell's law:

$$\theta_{\text{out}} = \arcsin\left(\frac{n_{\text{core}}}{n_{\text{external}}}\sin\theta_c\right) \tag{2.6}$$

Because this process can also be applied to the input, the maximum angle at which the light can enter the fibre and be accepted θ_{acc} can be found in a similar manner:

$$\theta_{\text{acc}} = \arcsin\left(\frac{n_{\text{core}}}{n_{\text{external}}}\sin\theta_c\right) \tag{2.7}$$

If the external medium is air, then it is acceptable to consider $n_{external}$ equal to one as the speed of light in air is close to that in free space. The range of acceptable input angles bound by the acceptance angle is known as the cone of acceptance. For convenience, the property known as the Numerical Aperture NA is the sine of this angle:

$$\mathrm{NA} = \sin\theta_{\mathrm{acc}} = n_{\mathrm{core}} \sin\theta_c \tag{2.8}$$

The numerical aperture can also be found by:

$$\mathrm{NA} = \sqrt{n_{\mathrm{core}}^2 - n_{\mathrm{cladding}}^2} \tag{2.9}$$

(Crisp 1996)

2.5 Optical Fibre

There are various types optical fibre types available. Conventional construction fibres are silica based but other options include plastic. Single-mode (SM) and multi-mode (MM) fibres are available depending on the application. Single-mode fibres have a thinner core and are designed to carry only a single mode of light. The thinner core means that the light does not have as far to travel across the width of the fibre, and less reflection is caused. Because of this, single-mode fibre fibre typically has a lower loss. Multi-mode fibre has a thicker core and allows more than one mode of light to be carried by the fibre and hence, more data can be carried. However, the thicker core means that more reflections occur down the length of the fibre, resulting in greater loss. This may limit the use of multi-mode fibres to shorter distances (Ohashi 2010).

Typically the core of a multimode fibre is 62.5μm in diameter while the core of a single mode fibre is 9μm. The cladding in either case is usually 125μm in diameter (Crisp 1996).

All optical fibres are described by the following parameters (Dakin & Culshaw 1988):

- Loss as a function of wavelength
- Numerical Aperture (sine of the maximum acceptance angle)
- Diameter of core, cladding and protective layers
- Properties of the cable including construction materials

2.6 Fibre Optic Sensors

The development of the laser and low loss optical fibre in the 1960s greatly increased the use of, and research into optical fibre for communications purposes. The 1970s introduced a new field of research utilising optical fibre technology for sensing purposes (Grattan & Sun 2000).

There are a number of benefits of fibre optic sensors over their traditional electronic counterparts. Some of these include: high sensitivity, low loss, resistance to chemically aggressive or corrosive environments, temperature resistance and low thermal conductivity. They can be designed to be compact and light weight and are suited to remote sensing applications, often requiring only a single lead to the sensor head. Finally, fibre optic sensors are immune to, and produce no electromagnetic interference (Ecke et al. 2012).

Despite the significant advantages of fibre optic sensors, they must still compete with their traditional electronic counterparts and are often more expensive. Advancement in technology is reducing the price gap between the two however, and fibre optic sensors often find niche applications where electronic sensors cannot be employed (Kersey 1996).

Some fibre optic sensors can display cross sensitivity between measurands, in particular, temperature fluctuation. Careful calibration, or using fibres of differing temperature sensitivity to measure the physical parameter of interest simultaneously can be used to offset this effect. Use of fibre such as phonic crystal fibre which is less sensitive to temperature can also reduce cross sensitivity significantly. The cross sensitivity of fibre optic sensors has otherwise been proven useful in measuring multiple physical parameters at once such as temperature and strain (Byeong Ha, Young Ho, Kwan Seob, Joo Beom, Myoung Jin, Byung Sup & Hae Young 2012).

2.6.1 Measurand Interface

The main division in measurand interfaces is between intrinsic and extrinsic interaction (Kersey 1996).

Intrinsic interaction has the measurand interacting with the fibre itself and hence the

light travelling inside the fibre is modulated by the physical parameter being measured. An example of intrinsic interaction would be strain which physically lengthens the fibre, hence causing a phase change in the light travelling in the fibre. Intrinsic operation may require that the fibre undergo additional processing such as machining or Bragg grating to enhance or permit its use in measuring some physical parameters. This process can be difficult or costly (Byeong Ha et al. 2012).

Contrasting this is extrinsic interaction which sees the measurand interact with an external component which in turn modulates the light. An example of extrinsic interaction would be an external mirror whose mechanical properties are altered by the measurand. The light reflected off this mirror is modulated by this interaction and is then directed into the optical fibre. Extrinsic operation has the disadvantage of difficulty with aligning external components or reduced sensitivity due to loss while light travels outside the fibre (Byeong Ha et al. 2012).

2.6.2 Fibre Optic Sensor Modulators

Modulator here refers to the parameters of the light travelling inside the fibre which the measurand can interact with. There are many modulators and the following section divides these into analogue and digital. It is important to note that many of these ultimately come back to being detected as changes in intensity, as the output of the photodetector operates only on light intensity.

Analogue

Intensity is modulated via a mask which alters the aperture and transmission through an extrinsic sensor. Intensity modulation may instead use a movable mirror to reflect light back into the fibre. Devices such as these often suffer from poor stability (Dakin & Culshaw 1988).

Phase, which is typically measured interferometrically, can be one of the most sensitive ways of measuring physical change. Usually this is achieved by measuring phase differences in two lengths of optical fibre, one the control arm, and the other the test arm which is subjected to change (Dakin & Culshaw 1988).

Polarisation is used in fibre optic sensors in a similar manner to interferometry. Light is transmitted along the two primary polar axes in a single medium. While travelling, the property being measured must only affect one polar plane. A polarisation analyser at the receiving end of the transmission medium detects the differences between the two polar axes (Dakin & Culshaw 1988). Fibres which display birefrigent properties are particularly useful for this type of sensor (Byeong Ha et al. 2012).

Colour of light (or frequency) has been shown useful as a modulator. The most successful example of this form of sensor is temperature sensitive luminescence. This can be achieved with optically excited phosphors, semiconductor and similar materials (Dakin & Culshaw 1988).

Digital and Others

On-Off Intensity is a typical digital modulator which can also be applied to light. The 'off' signal is better represented by a small intensity which indicates the system is still operational (Dakin & Culshaw 1988).

Modulation Frequency can be put on the light signal. This can be achieved through a mechanical oscillator whose frequency represents that of the measurand (Dakin & Culshaw 1988).

The decay time of excited inorganic phosphors can vary with environmental conditions. This can be utilised to measure these environmental factors such as temperature (Dakin & Culshaw 1988).

Hybrid Systems can be implemented through use of a traditional electronic sensor with a fibre optic transmission system. The output of the transducer modulates the emitting diode so that its signal is transmitted in light. This can be used to take advantage of the electromagnetic immunity of the fibre optics for at least the transmission of the signal, and will appear to the receiver exactly the same as a fibre optic sensor (Dakin & Culshaw 1988).

2.6.3 Components of Fibre Optic Sensors

This section briefly discusses the components which are common to all fibre-optic sensors: optical fibre, optical sources and optical detectors. The specifications which can be used to described these components are discussed. Other components which allow the measurand to modulate the light signal will be specific to the application.

Optical Fibre and Fibre Optic Components

There are several types of optical fibre available; multi mode and single mode fibres may be appropriate in fibre-optic sensors, but this vary with sensing application. The material that the fibre and its cladding are made out of will also vary depending on the application.

The construction of specialised optical fibres may be necessary for some applications. This might include the use of birefringent materials which refract light differently in each of the polar planes or the insertion of mirrors or Bragg gratings into the fibre itself to reflect the light inside the fibre.

In nearly all cases, additional fibre optic components will be required such as couplers and isolators.

Optical Sources and Detectors

Optical sources and detectors are classified primarily by wavelength. For sources, a minimum output power is provided while detectors will have a maximum input power. Details on stability with time and temperature will usually be given as well (Dakin & Culshaw 1988).

Signal Processing

Signal processing components are often required to gain meaningful information from the data provided by the sensor. Signal processing varies greatly with application but is essentially used to increase the quality of the output of the sensor. Some signal

processing may be required to compensate for non-linearity of certain sensing applications or enhance sensitivity and selectivity. A lock-in amplifier, which can be used to extract a signal in extreme background noise, is particularly useful for the latter of these purposes (Dakin & Culshaw 1988).

2.7 Interferometry

The basic concept of interferometry is the use of interference patterns from two superimposed waves to determine information about the waves. In fibre optic sensing, interferometry is usually used to determine the phase difference between two optical paths which provides information about the environmental factor being measured (Dyson 1970).

2.7.1 Interference of Light

It is known that light is part of the electromagnetic spectrum. As such it can be represented as a vector field. When two such fields (two sources of light) are superimposed on one another, the resulting field is the vector addition of the two. When the vector sum is found to be greater in amplitude than either of the two waves, the interference is said to be constructive. When the vector sum is found to be lesser in amplitude than the two waves, the interference is said to be destructive (Dakin & Culshaw 1988).

2.7.2 Interferometer Configurations

This section covers the main types of interferometer configurations used in optical fibre sensors. There are more interferometer configurations (such as the Jamin interferometer and Rayleigh's refractometer) which have been excluded due to being impractical, or varying only slightly from those discussed (Dyson 1970). An example of how each interferometer can be implemented using fibre-optics is also presented. In most cases, there are many more methods of constructing the interferometer in fibre-optics than shown.

Mach-Zehnder

A diagram of the Mach-Zehnder Interferometer is shown in Figure 2.1. Using a partially reflective mirror (Beam Splitter 1), the Mach-Zehnder configuration separates a single beam of light into two paths, the reference beam, and the sensing beam. The sensing beam is subjected to some external influence of interest, to which the reference beam remains unexposed. This results in a phase shift in the reference beam, and hence a phase difference between the two. The beams are recombined using a second partially reflective mirror (Beam Splitter 2) and the resulting interference can be viewed from the observation point (Françon 1966).

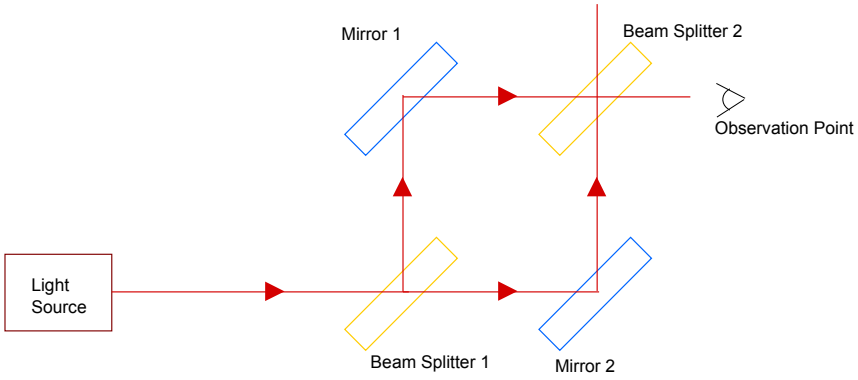

Figure 2.1: A diagram showing a Mach-Zehnder interferometer (Source: Author).

The Mach-Zehnder interferometer can be implemented in optical fibre components using a 50/50 coupler to divide the signal from an optical source into two lengths of optical fibre. The paths are then recombined by a second 50/50 coupler. The second 50/50 coupler equally divides the power of this signal into its two leads so it can be detected on either one by a photodetector (Byeong Ha et al. 2012).

A diagram of a fibre optic Mach-Zehnder interferometer is shown in Figure 2.2.

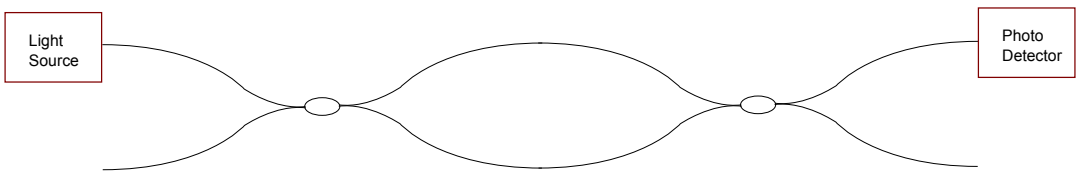

Figure 2.2: A diagram showing a Mach-Zehnder interferometer constructed from fibre-optic components (Source: Author).

Michelson

A diagram of a Michelson interferometer is shown Figure 2.3. The Michelson Interferometer, similar to the Mach-Zehnder, has a single beam split into two paths by a partially reflective mirror (Beam Splitter 1). However, these two paths are reflected back into the same partially reflective mirror by fully reflective mirrors (Mirror 1 and 2). The observer views the partially reflective mirror from the remaining side where the two beams are recombined. One arm serves as a reference and the other is subjected to external influence. The recombined beam shows interference caused by the phase change in the sensing arm (Françon 1966).

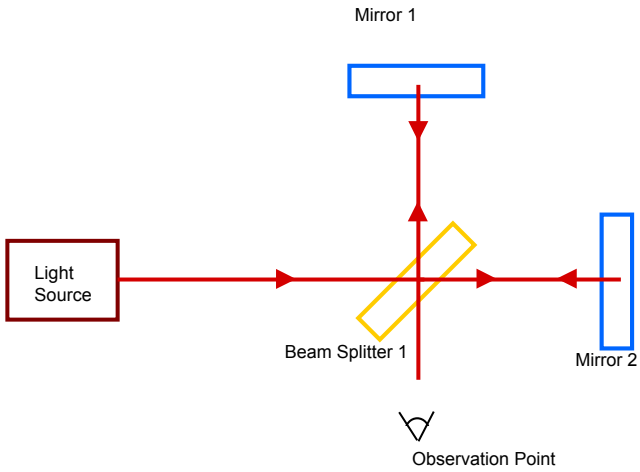

Figure 2.3: A diagram showing a Michelson interferometer (Source: Author).

The fibre-optic construction of the Michelson interferometer is similar to the Mach-Zehnder in that a source is put onto two leads joined by a 50/50 coupler. The difference being that the ends of these leads are terminated by a reflective surface (such as a fibre-optic retroreflector) which reflects the beams back to the coupler where they are recombined and a detector can read the interference as an output. Again, one of the arms acts as a reference with the other as thesensing arm (Yin et al. 2010).

A diagram of a fibre optic Michelson interferometer is shown in Figure 2.4.

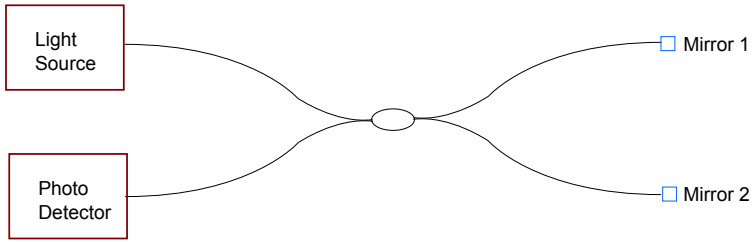

Figure 2.4: A diagram showing a Michelson interferometer constructed from fibre-optic components (Source: Author).

Sagnac

The Sagnac interferometer uses a partially reflective mirror to split a single beam into two; however these two beams share the same path. This is implemented in a ring formed by mirrors. One beam which is reflected by the partially reflective mirror travels the ring in one direction, while the beam which passes through the mirror travels the ring in the opposite direction. The two beams are recombined at the same partially reflective mirror and the observer views the interference that appears on the remaining side. The phase difference between the two may be caused by rotating the loop so that the light in one path has further to travel. This is how the Sagnac interferometer can act as a gyro scope (Culshaw 2006).

A diagram of a Sagnac interferometer is shown in Figure 2.5.

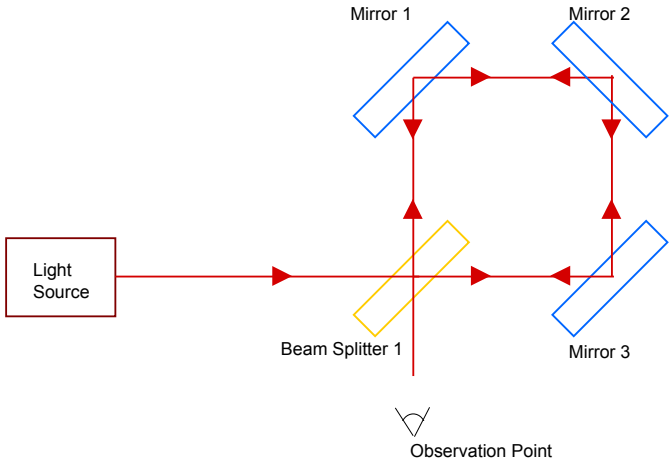

Figure 2.5: A diagram showing a Sagnac interferometer (Source: Author).

The full fibre Sagnac interferometer consists of single source which is passed onto a single length of optical fibre which is looped back onto itself. Before passing onto the loop, the light is polarised such that the perpendicular planes travel around the loop in opposite directions. A detector is coupled onto the same point as the source where the counterpropagating are recombined so that the interference can be detected (Culshaw 2006).

A diagram of a fibre optic Sagnac interferometer is shown in Figure 2.6.

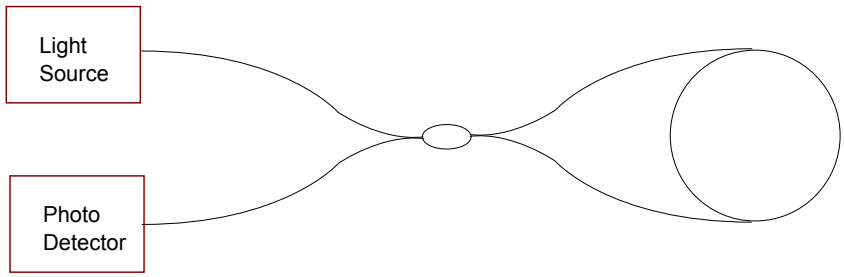

Figure 2.6: A diagram showing a Sagnac interferometer constructed from fibre-optic components (Source: Author).

Fabry-Perot

The Fabry-Perot interferometer passes a single beam of light through a partially reflective mirror and across a cavity (often referred to as a Fabry-Perot etalon) to a second partially reflective mirror. This causes the beam to reflect back and forth across the cavity many times. The cavity is where the external influence is applied. The interference can be viewed from behind either mirror where the multiple reflected beams are focused into a single beam by a lens. The effect is that each reflection reinforces the interference giving a clearer result than a single interfering beam (Yin et al. 2010).

A diagram of a Fabry-Perot interferometer is shown in Figure 2.7.

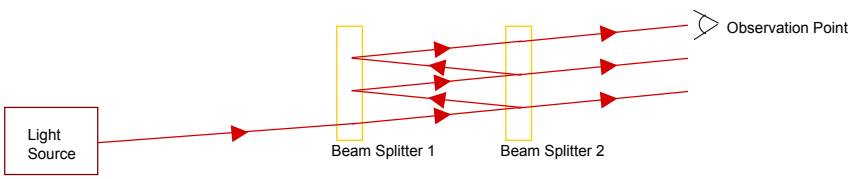

Figure 2.7: A diagram showing a Fabry-Perot interferometer (Source: Author).

There are several ways which the Fabry-Perot can be constructed with fibre optic components. Intrinsically, partially reflective sections can be added to the fibre itself to form the Fabry-Perot etalon. Alternatively, one end of the Fabry-Perot etalon can be formed using external components at the end of the optical fibre (Yin et al. 2010).

A diagram of two possible intrinsic fibre optic Fabry-Perot interferometer configurations is shown in Figure 2.8. Diagram (a) shows an optical fibre with an internal mirror and a partially reflective end forming the Fabry-Perot etalon. Diagram (b) shows an optical fibre with two internal mirrors forming the Fabry-Perot etalon.

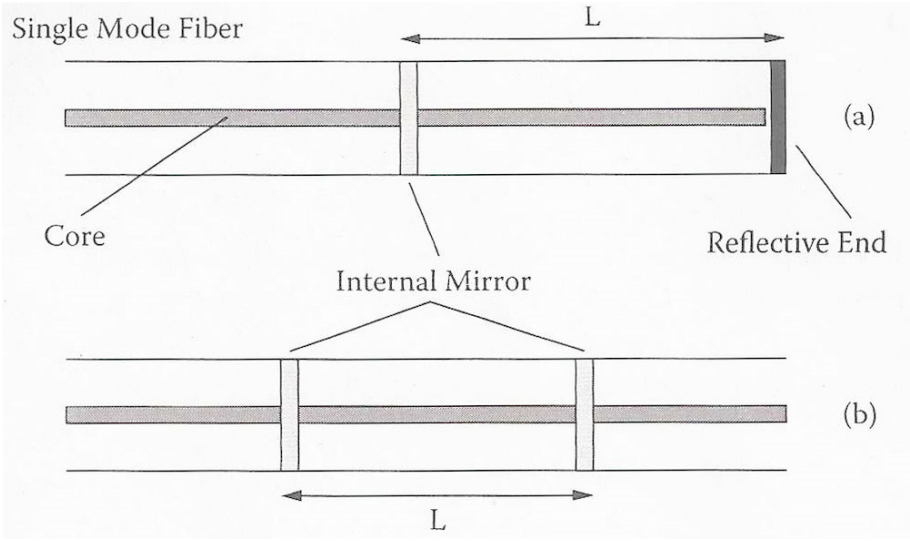

Figure 2.8: A diagram showing an intrinsic implementation of a Fabry-Perot interferometer in fibre-optic components (source: Yin et al. (2010)).

A diagram of one possible extrinsic fibre-optic Fabry-Perot interferometer configurations is shown in Figure 2.9. The Fabry-Perot etalon is formed between an optical fibre with a reflective end and an external reflective diaphragm.

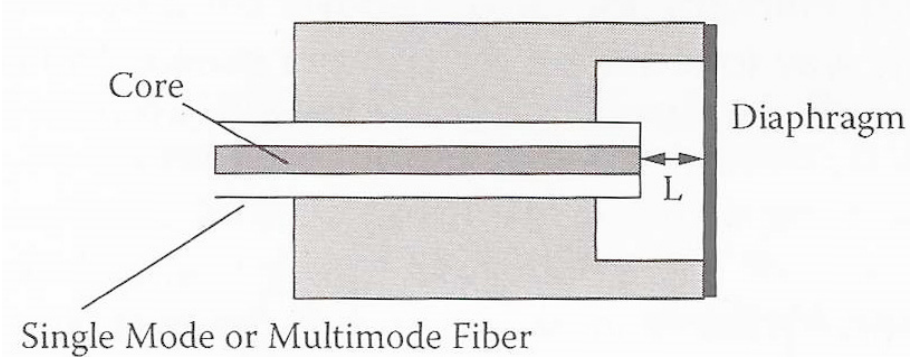

Figure 2.9: A diagram showing an extrinsic implementation of a Fabry-Perot interferometer in fibre-optic components (source: Yin et al. (2010))

2.7.3 Demodulating Interferometer Output

When the two paths of the interferometer are recombined, the result is the superposition of the two signals which are of the same frequency, with one including a phase shift (Culshaw 1984). This is represented mathematically in 2.10.

$$E_{tot} = E_1 \sin \omega t + E_1 \sin(\omega t + \phi) \tag{2.10}$$

(Culshaw 1984)

Where E_1 and E_2 are the amplitudes of the signals being combined, ω is the angular frequency of the light from the optical source and ϕ is the instantaneous phase change in the sensing arm.

The detector is matched to the source frequency ($\sin \omega$) and responds to variations in the intensity at the receiving end. Therefore, its output $v(t)$ will vary as with the phase difference as in (2.11) (Culshaw 1984).

$$v(t) \propto 1 + \cos \phi(t) \tag{2.11}$$

(Culshaw 1984)

2.8 Design Implications

The review of the operation of fibre-optics in this chapter provided an analysis of how this technology can be utilised for sensing applications. This leads to many ways in which the measurand can interact with the optical fibre for sensing applications including intensity, phase, colour and more. The separation between intrinsic and extrinsic interaction has been discussed and each is useful in their own right. Interferometry was discussed due to its usefulness in enhancing fibre-optic sensors. Several interferometer configurations have been shown and each serves as an option to base the fibre-optic microphone design on. This information will aid in the design of the fibre-optic microphone.

Chapter 3

Photoacoustic Spectroscopy

This chapter discusses photoacoustic spectroscopy, the application for the fibre-optic microphone designed in this project. A brief background on photoacoustic spectroscopy will be given, followed by a description of how it can be used to detect gases. Lock-in amplifiers are useful in extracting the output of a photoacoustic spectroscopy system, so this piece of equipment is discussed. Finally, the impact this application will have on the design will be considered.

3.1 Background of Photoacoustic Spectroscopy

In 1880 Alexander Graham Bell discovered that a thin disc would produce sound when exposed to a light source which was mechanically chopped. This effect was later explained by researchers at Bell Labs and formed the basis of photoacousitc spectroscopy (Haisch & Niessner 2002).

Photoacoustic spectroscopy is considered a photothermal technique as it utilises the heat resulting from exposing a sample to light. The increase in temperature will also cause the material to expand. If the light is intensity modulated, then the material will expand and contract cyclically which causes a periodic pressure change to occur at the frequency at which the light is oscillated. This is an audio signal which can be detected using a microphone (Ball 2006).

3.2 Photoacoustic Detection of Gases

Photoacoustic spectroscopy can be applied to all phases of matter, but has proven to be particularly useful in trace gas detection (Ball 2006). Gases can be detected according to their absorption spectra. A gas of any molecule has a fingerprint spectrum of light that it will absorb and convert to heat energy. This is the same spectrum of light that the gas will emit when heated to the point that it produces light. These spectra are known through previous experimentation. In photoacoustic spectroscopy, a light source can be selected such that its wavelength is absorbed by the gas in question. This could be a narrow band laser light source or a broadband light source which is put through a filter to extract only the desired wavelength. The latter of the two will inherently be less powerful but has the advantage of being the cheaper option (Harren, Cotti, Oomens & Hekkert 2000).

In photoacoustic detection of gasses, the vessel in which the gas is excited is called the photoacoustic cell. Ideally the cell should aid in isolating the gas from interfering electromagnetic and light signals, which may also excite the gas and induce pressure waves. The cell should also be kept isolated from other acoustic signals. Placement of the light source and sensing head/membrane of the microphone will also need to be considered. The cell can be constructed such that its resonant frequency matches that of the sound produced, amplifying the signal (Harren et al. 2000).

This technique provides both an indication of the presence of the gas in question, and also an indication of how prevalent it is in the sample. If no audio tone is produced, then no gas molecules whose absorption spectra matched the laser used are present. If a tone is produced, its amplitude or volume is proportional to the number of molecules in the sample (Harren et al. 2000).

3.3 Resonance

An object will vibrate with greater amplitude at certain frequencies than others in an effect known as resonance. These frequencies are the same that the object naturaly tends to vibrate at, and are known as its resonant frequencies. In simple systems such as a string, or a cylinder of air, these frequencies can be predicted (Giancoli 1991).

The photoacoustic cell can be viewed as a column of air. If both ends of the cylinder are open, the fundamental resonant frequency can be found by:

$$f_{\mathrm{r(open)}} = \frac{v}{2l} \tag{3.1}$$

(Mayfield, Parham & Webber 1984)

Where $f_{\mathrm{r(open)}}$ is the fundamental resonant frequency of a cylinder with open ends, v is the speed of sound and l is the length of cylinder.

In the case of a cylinder with one end closed and the other open, the fundamental resonant frequency can be found by:

$$f_{\mathrm{r(closed)}} = \frac{v}{4l} \tag{3.2}$$

(Mayfield et al. 1984)

Where $f_{\mathrm{r(closed)}}$ is the fundamental resonant frequency of a cylinder with one closed end, v is the speed of sound and l is the length of cylinder.

Further resonant frequencies occur at the harmonics of the fundamental resonant frequency, and can be found by multiplying the fundamental frequency by any positive integer (Mayfield et al. 1984). The speed of sound in air varies in different materials, but also varies with temperature, pressure and humidity in air. For a temperature of 20°c at sea level, the speed of sound in air is approximately 343 m/s (Giancoli 1991). This value serves as a good approximation when temperature, pressure and humidity are unknown.

3.4 Signal Processing

The audio signal received by the microphone will need to undergo some processing in order to extract the desired frequency. One option is Fourier analysis of the signal from the microphone. This will produce a spectrum output which can be examined to discern if a peak exists at the frequency in question. Alternatively, as the audio frequency is known, a lock-in amplifier can be used and locked to the modulating frequency of the

light source. This method immensely increases the sensitivity of the device and almost completely eliminates the effect of noise.

3.5 Lock In Amplifiers

Lock-in amplifiers amplify only signals of a given carrier frequency. This is achievable even amongst noise of a much greater amplitude then the carrier signal, or when the signal to noise ratio (SNR) is extremely low. To do this, the lock-in amplifier is provided with a reference signal to which the incoming signal is compared. Alternatively, the frequency of the internal oscillator can be set without a reference. Signals on a carrier with the same frequency as the reference are preserved while all others (noise) are eliminated. It does this via the use of a Phase Sensitive Detector (PSD) (Banuelos-Saucedo & Ozanyan 2012).

The operation of the PSD is a homodyne detection technique. This is similar to heterodyne processing used in radiowave demodulation, with the exception that the incoming signal and the reference signal are of the same frequency. The incoming signals are multiplied with the reference signal. This produces secondary signals at the sum and difference of the reference and incoming signals (Banuelos-Saucedo & Ozanyan 2012). Mathematically, this is:

$$V_{\mathrm{PSD}} = V_{\mathrm{ref}} \sin(\omega_{\mathrm{ref}} + \theta_{\mathrm{ref}}) V_{\mathrm{sig}} \sin(\omega_{\mathrm{sig}} t + \theta_{\mathrm{sig}}) \tag{3.3}$$

$$V_{\mathrm{PSD}} = \frac{1}{2} V_{\mathrm{ref}} V_{\mathrm{sig}} \Big[\cos((\omega_{\mathrm{ref}} - \omega_{\mathrm{sig}})t + (\theta_{\mathrm{sig}} - \theta_{\mathrm{ref}})) + \cos((\omega_{\mathrm{ref}} + \omega_{\mathrm{sig}})t + (\theta_{\mathrm{sig}} + \theta_{\mathrm{ref}})) \Big] \tag{3.4}$$

(Banuelos-Saucedo & Ozanyan 2012)

Where V_{PSD} is the voltage output of the PSD, V_{ref} is the voltage of the reference signal, ω_{ref} is the angular frequency of the reference signal, θ_{ref} is the phase change in the reference signal, V_{sig} is the voltage of the input signal, ω_{sig} is the angular frequency of the input signal, θ_{sig} is the phase change in the input signal.

If these resulting sum and difference frequencies are passed through a high quality low-pass filter, no signals remain except for the case where $\omega_{\mathrm{ref}} - \omega_{\mathrm{sig}} = 0$ (i.e. the signal

frequency is the same as the reference frequency). In this case, because $\cos(0) = 1$, the signal amplitude V_{sig} is preserved. As an alternative to the low pass filter, the product signal can be integrated over a period much longer than that of the reference signal. This results in a value equal to the amplitude of any input signal with a frequency matching the reference while all others are attenuated (Banuelos-Saucedo & Ozanyan 2012).

3.6 Interferometers in Fibre-Optic Microphones

Previous research into microphones based on fibre-optic sensors has been successful. The following are several examples, arranged by the construction type, which show how microphones can be constructed using each interferometer configuration discussed.

3.6.1 Michelson Interferometer

The article 'Photoacoustic Detection of Trace Gases with an Optical Microphone' (Breguet, Pellaux & Gisin 1995) describes the construction of two separate configurations. The first is based on the Michelson interferometer. The sensor head is a diaphragm which is built in to an aluminium cylinder which acts as a photoacoustic resonator cell. The gas in the cell is excited by a CO_2 laser which causes a heat increase and in turn, a pressure wave. The laser is pulsed so that a sound wave is formed and is detectable by the microphone. The Michelson interferometer based microphone was found to be more sensitive then a conventional microphone in detecting a response from the resonator cell (Breguet et al. 1995).

3.6.2 Sagnac Interferometer

The article 'Photoacoustic Detection of Trace Gases with an Optical Microphone' (Breguet et al. 1995) also describes a fibre optic microphone constructed from a Sagnac interferometer. A 4.5km loop of optical fibre was used in order to create a delay in phase difference between the counter-propagating light modes. The Michelson based configuration was three times as sensitive as the Sagnac (Breguet et al. 1995).

3.6.3 Fabry-Perot Interferometer

'Extrinsic Fabry-Perot Interferometer Fiber-Optic Microphone' (Furstenau, Horack & Schmidt 1998) details a system of microphones based on an extrinsic Fabry-Perot interferometer. A system which employs six sensors is used for monitoring ground traffic at the Brunswick airport. The sensors are deployed remotely and are each linked back by a single mode fibre to a central control room. Plane types can be identified by spectrum analysis of engine noise as detected by the sensors.

The Fabry-Perot etalon is formed by a reflective fibre which is glued into a ferrule on the end of the optical fibre itself. A membrane is vibrated by the audio source and mechanically transfers the variation to the Fabry-Perot etalon. The optical source and detector are both coupled to the single mode fibre at the control room. The change in length in the etalon causes phase modulation, and an interference pattern which is reflected back down the optical fibre to the control room.

The microphones were tested under lab conditions in an anechoic chamber as well as in realistic conditions, exposed to air vehicle engine noise. The results were promising and field testing revealed the differences in the audio spectra from the engine noise could be used to identify the aircraft (Furstenau et al. 1998).

3.6.4 Mach-Zehnder Interferometer

'Optical Fibre Mach-Zehnder Microphone' (Kruger & Theron 2007) describes a fibre optic microphone based on a Mach-Zehnder interferometer. The sensor head is constructed by gluing the optical fibre to a membrane made of solar film. The membrane is mounted on a hole cut into a metal dish. The reference arm is isolated from the sound source.

The microphone was used to record voice. Test results were compared to that of a conventional microphone which recorded audio simultaneously. Analysis revealed that the fibre optic microphone had a better response to higher frequencies, but displayed higher levels of noise below 200Hz. The fibre optic microphone also lacked the 50Hz hum present in the conventional microphone recording which highlights the electromagnetic immunity of the fibre optic microphone (Kruger & Theron 2007).

3.7 Design Implications

This chapter has covered photoacoustic spectroscopy and how it can be used in the detection of gases. As was discussed, the amplitude of the tone from the photoacoustic cell is representative of the number of molecules of the gas in question, so it is important that the microphone not only detects when a tone is present, but also the amplitude of the tone. It was shown that a lock-in amplifier can be an extremely useful component in a microphone system used in photoacoustic spectroscopy. Finally, an example was given of each interferometer implemented in a fibre-optic microphone. This provides several options for the design of the fibre-optic microphone in this project.

Chapter 4

Design of the Fibre-Optic Microphone

This chapter shows the design of the fibre-optic microphone. Based on the research in the previous chapters, the most appropriate interferometer configuration will be chosen to based the design on. A diagram of the design will be presented as well as a description of its operation.

4.1 Sensor Interface

Vibration from sound is able to interact with the fibre itself so no external components are necessary; this is a form of intrinsic interaction. When the vibration is transferred to the optical fibre, it causes it to expand and contract. When it expands, the length of the path which the light must travel is increased, causing a delay at the receiving end, and hence a phase change. As the fibre contracts, the phase change is reversed. When the expansion and contraction occurs at the frequency of the audio tone picked up by the optical fibre, the phases will shift at the rate of this vibration (Dakin & Culshaw 1988). This means the fibre-optic microphone will function on a form of phase modulation. This phase modulation can be hard to track, so an interferometer will be incorporated.

4.2 Interferometer Configuration

The interferometer configuration chosen for the design is the Mach-Zehnder. This configuration has been chosen as it offers high sensitivity and can be constructed from readily available fibre-optic components.

The Michelson interferometer could also be constructed from similar components. Lengths of optical fibre terminating in reflective ends are required for this configuration and are available for purchase. However, this configuration results in high levels of back reflection to the source, which greatly degrades performance (Yin et al. 2010).

The Sagnac interferometer has been extremely successful in its implementation as a gyroscope (Culshaw 2006). However, the Sagnac interferometer is not well suited to measuring acoustic pressure. The use of optical fibre with high birefringent properties or fibre Bragg gratings can expand the usefulness of the Sagnac interferometer to measure other properties, but these require specialised techniques to create, hence increasing complexity and cost (Byeong Ha et al. 2012). As seen in the example of a fibre-optic microphone constructed from a Sagnac interferometer, a 4.5km length of fibre was require to introduce a delay between the phase change in the counter-propagating light paths (Breguet et al. 1995). This increases cost and loss, making this option less sensitive then others.

The Fabry-Perot interferometer has previously been used to construct fibre-optic microphones. However, these are very difficult to construct. Extrinsic Fabry-Perot interferometers require external components. Because the diameter of optical fibre is on the scale of μm, external components can be very difficult to align with the optical fibre. An intrinsic Fabry-Perot interferometer is also an option, but requires fibre Bragg gratings or reflective surfaces to be spliced into the fibre itself. This is also made difficult due to the extremely small diameter of the optical fibre. This makes the Fabry-Perot interferometer the most complex or costly option (Byeong Ha et al. 2012).

The Mach-Zehnder is the best choice to base the fibre optic microphone on. It can be constructed from readily available components and does not require light to be reflected back down the fibre.

4.3 Design

The design of the microphone is shown in Figure 4.1.

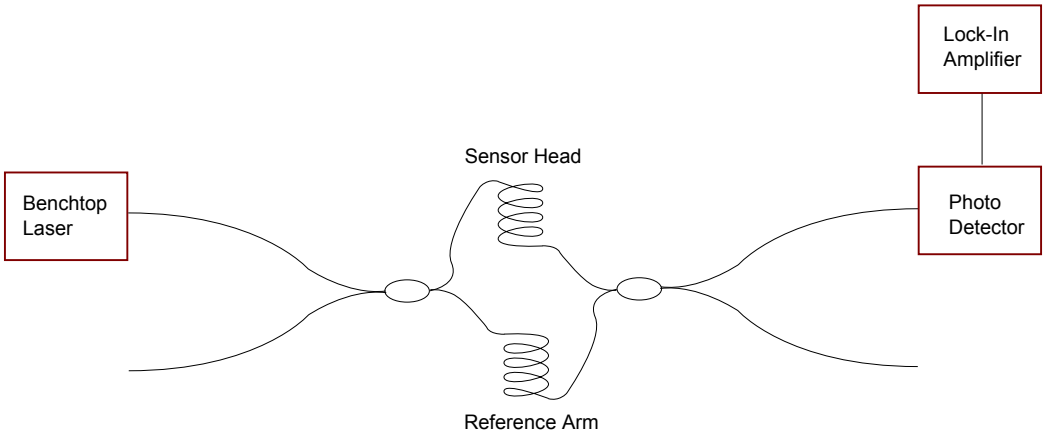

Figure 4.1: A diagram showing the proposed fibre-optic microphone design(Source: Author).

A bench top laser provides the light source. The Mach-Zehnder interferometer is formed using two cascaded 2x2 couplers. Here, one path acts as the sensing arm and the other as a reference. An intrinsic approach will be implemented, in that the audio will interact with the fibre of the sensing arm itself. The reference arm is kept isolated from the audio source. The output of the interferometer (the recombined signal) is fed to the photo detector. The output of the photo detector is then passed to the lock-in amplifier. The lock-in amplifier can be set to the frequency of interest, or a reference can be provided depending on the audio source.

4.4 Equipment

4.4.1 Optical Source

The optical source chosen for the construction is the Thorlabs S1FC Benchtop Laser. The model chosen for the construction of the fibre optic microphone produces light at a wavelength of 1550nm. It is fibre coupled with a single mode FC/PC output.

This source has an adjustable power output up to 1.5mW. This can be adjusted from 0mW to full power with a resolution of 0.01mW and the current value is displayed

on its 3.5 digit display. The power output is stable to ±0.05dB over 15 minutes or to ±0.1dB over 24 hours after a 1 hr warm up at and ambient temperature of 25°C ±10°C.

The power out can also be modulated by a signal connected to the 'mod in' input. The modulating signal range is 0 to 5V and should be DC or sin wave only. A modulation frequency of up to 5Hz is acceptable for full range modulation, or up to 30kHz for small signal input (*Thorlabs S1FC Fibre Coupled Laser Source Operating Manual* 2013).

Figure 4.2 shows the Thorlabs S1FC Benchtop Laser Source.

Figure 4.2: The Thorlabs S1FC Benchtop Laser used as the light source in the fibre-optic microphone design (source: Thorlabs S1FC Manual).

4.4.2 Photodetector

The photodetector selected for the project is the Thorlabs PDA8GS. This photodetector is fibre coupled and accepts both single mode and multi mode fibre inputs. The wavelength range for this photodetector is between 700nm and 1650nm with a peak sensitivity between 1100nm and 1550nm. This makes it suitable for use with the Thorlabs S1FC Benchtop Laser Source at a wavelength of 1550nm. However, the maximum constant input power for the PDA8GS is 1mW which is less than the maximum output of the S1FC, so care must be taken not to exceed 1mW constant use. At 1550nm the sensitivity of the Thorlabs PDA8GS is -20 dBm. The Thorlabs PDA8GS has an 50Ω SMA output connector (*Thorlabs PDA8GS Fibre Coupled Photodetector Specification Sheet* 2010).

Figure 4.3 shows the Thorlabs PDA8GS Photodetector.

Figure 4.3: The Thorlabs PDA8GS photodetector used to detect the recombined light signal at the output of the interferometer (source: Thorlabs PDA8GS Manual).

4.4.3 Couplers

The couplers used will be Thorlabs 10202A 2x2 50:50 couplers. These couplers are single mode with FC/PC connectors and are suitable for both 1550 and 1310nm. This means they are suitable for the light source chosen for the design. They have an insertion loss of 3.8db and an excess loss of 0.2dB. The leads out of the coupler are 1m long had have 900μm diameter jackets. (*Thorlabs 2 x 2 Single Mode Fiber Couplers and Taps* 2013).

Figure 4.4 shows the Thorlabs10202A 2x2 50:50 Coupler.

Figure 4.4: The Thorlabs10202A 2x2 50:50 coupler used to construct the Mach-Zehnder interferometer (source: Thorlabs10202A Manual).

Figure 4.5 shows how the Thorlabs10202A 2x2 50:50 combines two signals and splits the power of the combined signal evenly between two ports.

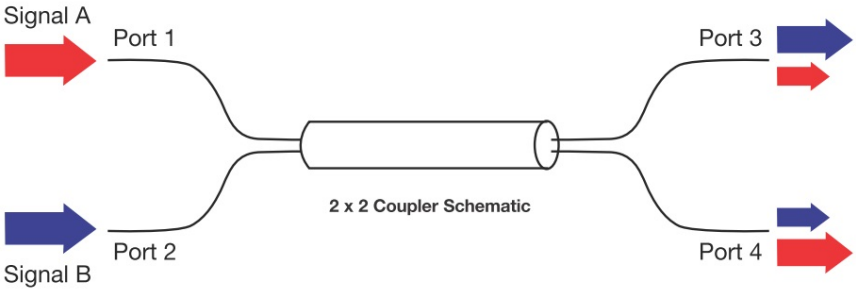

Figure 4.5: A diagram of the Thorlabs10202A 2x2 50:50 coupler showing how the signals on its input are combined, then split evenly between two ports (Source: Thorlabs10202A Manual).

4.4.4 Lock-In Amplifier

The lock in amplifier is an AMETEK Signal Recovery Model 7270. This lock-in amplifier has a frequency range of 0.001Hz to 250kHz with sensitivity ranging from 2nV to 1V full-scale. The reference signal can be supplied to the reference input, or the oscillator frequency can be manually. Two signal inputs are provided, and time constant can be adjusted from 10μs to 100ks (*AMETEK Model 7270 DSP Lock-in Amplifier Instruction Manual* 2010).

Figure 4.6 shows the AMETEK Signal Recovery Model 7270 lock-in amplifier.

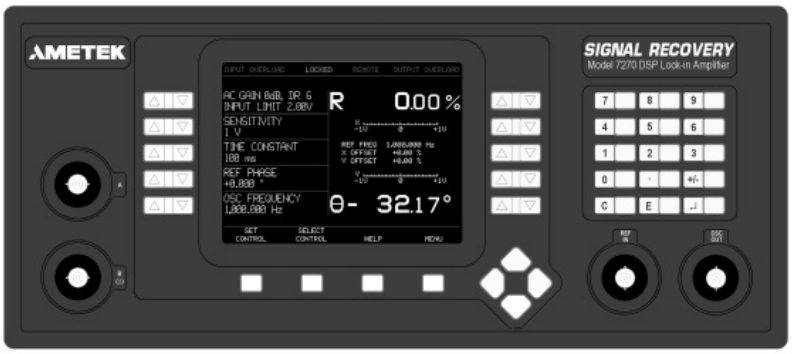

Figure 4.6: The front panel of the AMETEK Signal Recovery Model 7270 used to detect the tone signal in the output of the interferometer (source: AMETEK 7270 Manual).

4.5 Sensor Head

As the design is intrinsic, the audio must interact with the fibre in the sensing arm. To achieve this, the fibre of the sensing arm is coiled around a PVC former. Duct tape tightly wrapped around the coil is used to fix the fibre to the PVC. A tone in the air surrounding the former will cause it to vibrate. This vibration will then be transferred to the optical fibre of the sensing arm. The sensor head is shown in Figure 4.7.

Figure 4.7: An image showing the sensor head of the fibre-optic microphone. The optical fibre is coiled around the PVC former and fixed firmly in place with duct tape (Source: Author).

The connection point of the two couplers is in the centre of the sensing arm. This connection is housed in a metal project box to isolate it. The coil is then formed by doubling up the fibre from this connection, and winding back from this point to incorporate as much of the sensing arm as possible. This whole unit is set upon a piece of foam to isolate it from vibrations in the bench top itself. Figure 4.8 shows this arrangement. The left image shows the coil before it is taped to the former, and the connection point in the centre of the sensing arm. The right image shows the coil once it is taped to the former, and the connection point housed in a project box.

The PVC former is 100mm in length and has a nominal diameter of 20mm. Its inner diameter is 23.7mm and outer diameter is 26.8mm. The sensing part of the fibre has been doubled up and wrapped around the former 5 times, resulting in 10 loops of optical fibre. The width the entire coil across the length of the PVC former is 18mm. The total length of fibre in the coil (the sensing length) is 842mm. The closest edge of the coil is 12mm from the end of the PVC former.

Equation (3.1) which is used to calculated the fundamental resonant frequency of a open ended cylinder of air is applicable to the sensor head. Using 343 m/s as an approximate value for the speed of sound, the fundamental resonant frequency of the sensor head can be found.

$$f_{\text{fundamental}} = \frac{v}{2l} = \frac{343}{2 \times 0.1} = 1715Hz \tag{4.1}$$

Harmonic resonant frequencies occur at multiples of this value.

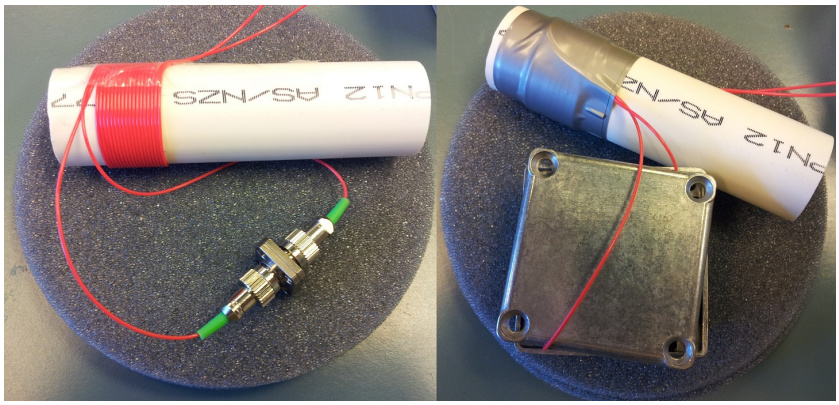

Figure 4.8: An image showing the sensor head arrangement. The left image shows the optical fibre coiled around the former before being fixed in place with duct tape. The right image shows the joint housed in a metal project box (Source: Author).

4.6 Reference Arm

To aid in isolating the reference arm, the fibre is loosely wrapped around a PVC former as shown in Figure 4.9.

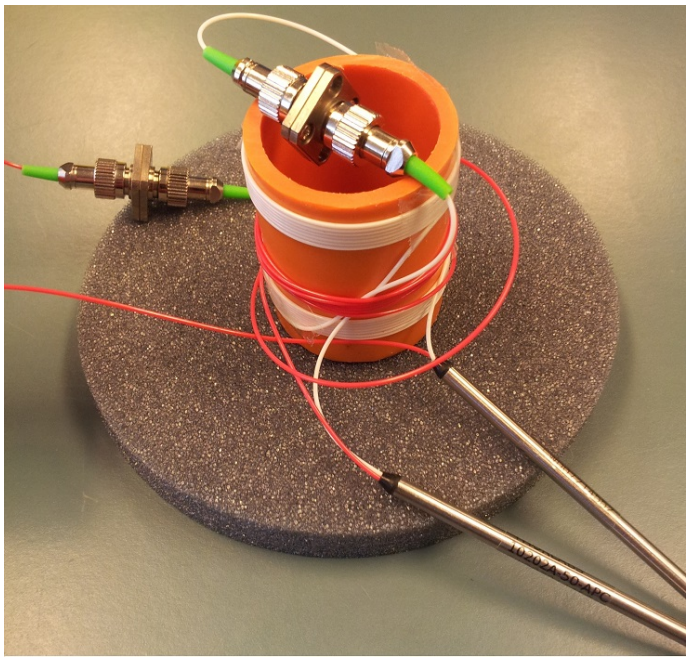

Figure 4.9: An image showing the reference arm loosely coiled around a PVC support (Source: Author).

This unit is then placed in a metal project box insulated with foam. Figure 4.10 shows this arrangement. A layer of foam is placed over the sensing arm as it is shown in Figure 4.10 before the lid is placed on top.

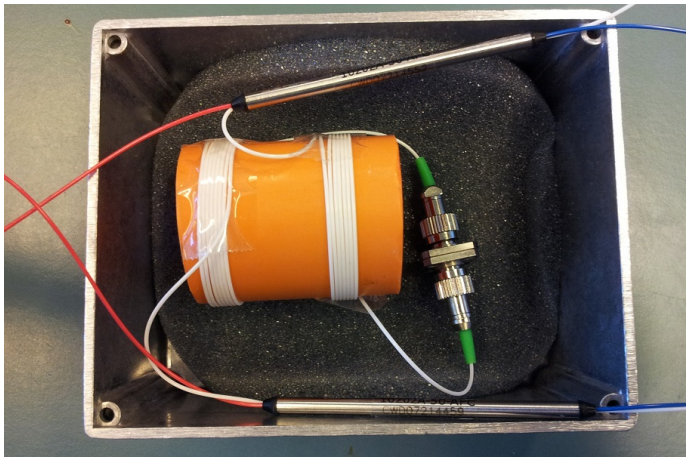

Figure 4.10: An image showing the reference arm housed in an insulated project box before the lid has been put in place (Source: Author).

4.7 Design Implementation

This chapter has proposed a fibre-optic microphone design. The fibre-topic microphone described in this chapter has been implemented as shown in figure 4.1 using the equipment listed in Section 4.4. A thorough evaluation of performance will take place on the constructed fibre-optic microphone. This testing will be described in the following chapter.

Chapter 5

Evaluation of Performance

This chapter covers the testing of the fibre-optic microphone and evaluation of its performance. The equipment used in testing the device and how it is configured will be covered first. Following this is a series of tests each with a description of method, display of results and discussion of results.

To show that the fibre-optic microphone is functioning and suitable for use in photoacoustic spectroscopy, it must be able to produce an output proportional to the volume of a tone which it is locked to. For the fibre-optic microphone, the output is regarded as the reading taken from the lock-in amplifier.

Initial testing will take place to ensure the fibre-optic microphone response, as read from the lock-in amplifier, is proportional to the tone at the locked frequency. The fibre-optic microphone will then be tested at a variety of frequencies to determine what effect frequency has on its response. The effect of the power level of the benchtop laser will be investigated by trialling a selection of power level settings. The final test will investigate the option of implementing a carrier by modulating the laser with a signal whose frequency is locked by the lock-in amplifier.

5.1 Testing Equipment

5.1.1 Function Generator

The function generator used in testing is the RIGOL DG4062 Function/Arbitrary Waveform Generator. This is a 2 channel generator which can produce a number of standard and arbitrary waveforms. The frequency range is adjustable from 1μHz to 60MHz with a resolution of 1μHz. Up to 20Mhz, the peak to peak amplitude of the output can be adjusted from 1mVpp to 20Vpp with a resolution of 1mV. This is much greater than the frequency range that will be necessary for testing. For all testing a sine function will be used.

Figure 5.1: An image showing the front panel of the RIGOL DG4062 Function/Arbitrary Waveform Generator (Source: RIGOL DG4062 Manual).

5.1.2 Sound Level Meter

The sound level meter used is the Larson Davis SoundTrack LxT1. The measurement range of the device is 39 to 140dB which is more than enough for the volumes levels that will be produced in testing.

The sound level meter allows frequency weighting to be applied. These weightings are perceptual based so that the frequency response would be similar to a human ear. This is not suitable for testing the fibre-optic microphone, so the Z weighting will be used. This is a flat frequency response weighting, so that the sound level meter reading is not weighted on frequency.

Figure 5.2: An image showing the Larson Davis SoundTrack LxT1 sound level meter (Source: Larson Davis SoundTrack LxT1 Manual).

5.1.3 Lock-In Amplifier Settings

As shown in Section 4.4.4, the lock-in amplifier used in the fibre-optic microphone is the AMETEK Signal Recovery Model 7270. The settings on the lock-in amplifier have a great impact on the test results. These are the time constant over which the signal on its input is integrated, and the sensitivity setting.

A lower sensitivity is better in order to achieve greater resolution. As will be seen in testing, the full scale variation of the fibre-optic microphone output is less than one mV, so a setting of 1mV or even less could be used. However, on this setting, the output displayed on the lock-in amplifier does not settle. This is likely due to small variations in the signal strength which are picked up at this sensitivity setting. A setting of 100mV provides resolution enough to differentiate sound level, but will also settle on a specific value after the settling time. For this reason, the sensitivity will remain at 100mV for all tests.

The time constant affects the accuracy of the output that the lock-in amplifier shows. A longer time constant will result in greater accuracy, but also a greater settling time must be allowed. For the fibre-optic microphone system, it was found that time constants of less than 10s produced varying results indicating inaccuracy on these settings, while time constants of 10s or more provided the same result, indicating no further accuracy would be gained by using these settings. Because of this, a time constant of 10s is used for all testing. In order to ensure the output has settled, a settling time of 40s is allowed before a reading is taken.

5.2 Curve Fitting

Fitting a curve to test data can be useful in showing the relationship between the test variables. As will be shown in initial testing, the fibre-optic microhpone exhibits an exponential response to the volume of a tone at the locked frequency. As such, it will be necessary to fit an exponential curve to the data. The MATLAB function fit() uses the method of least squares to fit a curve to a data set. This function allows the curve type to be specified. In this case, a single term exponential is appropriate and will be fit to the result data as appropriate. This method will be used for all curve fitting and it can be seen employed in Figure 5.4.

5.3 Experiment Setup

Figure 5.3 shows the configuration used to test the microphone. A speaker and function generator have been introduced. The output of the function generator is fed to both the speaker, and the reference input on the lock-in amplifier. The tone produced by the speaker will be transferred to the sensor head, and appear in the output of the photo detector. The lock-in amplifier will lock to the function generator frequency and display the amplitude of this frequency as received from the photo detector. This set up will be used for initial testing, frequency testing and power level testing.

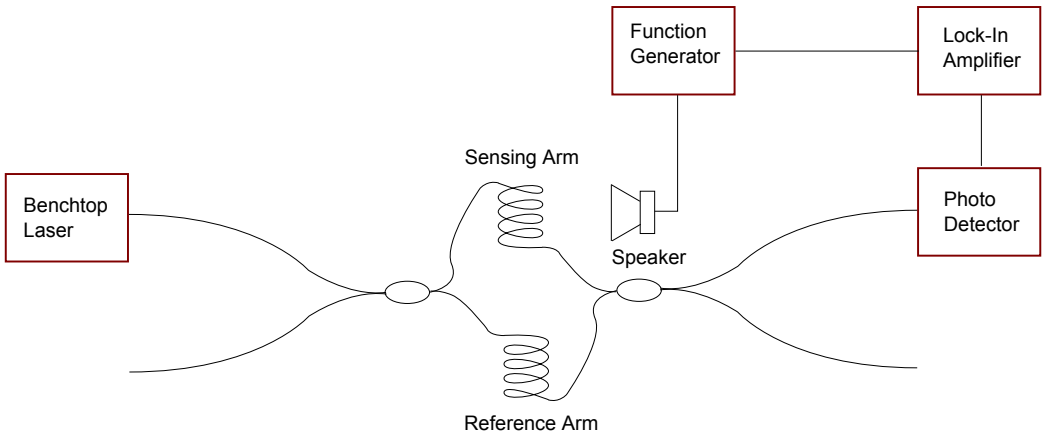

Figure 5.3: A diagram shown the experiment set up used for the first three experiments (Source: Author).

5.4 Initial Testing

In order to determine if the microphone will produce a response proportional to the volume of the audio it receives, the volume of the tone produced by the speaker will be stepped up incrementally. At each step, the lock-in amplifier measurement will be recorded.

5.4.1 Setup

The setup shown in Figure 5.3 will be used for this test.

5.4.2 Method

Procedure

1. Set the function generator to the desired frequency and the lowest amplitude step.
2. Disconnect the PC speaker so there is no tone. Allow the lock-in amplifier to lock to the signal and record the amplitude once it has settled. This is the measurement for 0V signal to the speaker.
3. Connect the speaker and record the amplitude once it has settled.
4. Increment the function generator voltage and record the amplitude once it has settled.
5. Repeat the previous step until the all voltage steps have been tested.

The test will be repeated three times, and the results averaged.

Test Parameters

Function Generator Frequency:	1kHz
Function Generator Voltage Range:	0 to 16V peak to peak
Voltage Step:	2V
Lock-In Time Constant:	10s
Settling Time:	40s
Laser Power:	0.5mW

5.4.3 Results

Table 5.1 shows the measurements taken over three tests as well as the average. Figure 5.4 shows the plot of the average calculated from the measured data, as well as an exponential curve fit to the data.

Table 5.1: Results of initial testing

Function Generator (V)	Test 1 (μV)	Test 2 (μV)	Test 3 (μV)	Average (μV)
0	0	0	0	0.00
2	10	0	0	3.33
4	30	20	10	20.00
6	20	10	20	16.67
8	20	20	60	33.33
10	120	70	50	80.00
12	80	110	70	86.67
14	90	120	90	100.00
16	190	170	110	156.67

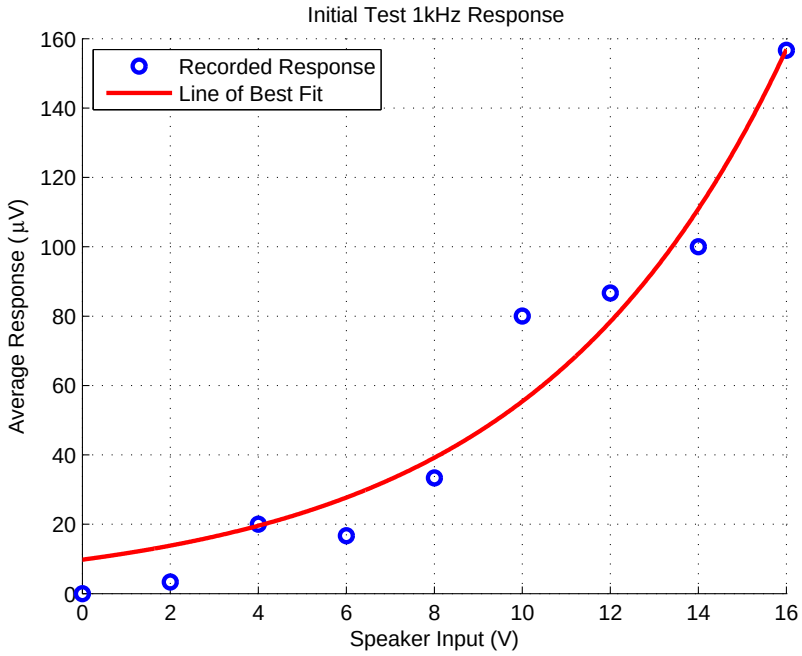

Figure 5.4: A plot of the results of initial testing, including data points and an exponential curve fit to the data.

5.4.4 Discussion

Initial testing shows that the device is working as expected. When no tone of the locked frequency is present, the lock-in amplifier always settles to zero. When a tone

of the locked frequency is present, the lock-in amplifier shows a response which is proportional to amplitude of the tone present. The curve of the data is exponential, so the microphone response has an exponential relationship to the volume of the tone. In practice, the exponential response would need to be accounted for when taking measurements with the fibre-optic microphone.

The result data is somewhat anomalous in that a few measurements show a decrease in the microphone output in response to an increase in tone volume. However, in general the microphone response increases exponentially with tone volume. This proves the concept of the fibre-optic microphone is successful, and suitable for use in photoacoustic spectroscopy.

5.5 Frequency Response

The response of the microphone over a selection of frequencies will now be tested. The range of frequencies it is possible to test is limited by the output ability of the speaker, so frequencies will be chosen between 500Hz and 20kHz.

In addition to measuring the response of the microphone as the voltage on the function generator is increased, at each voltage step, a reading will be taken with a sound level meter. This will provide a more direct comparison for the fibre-optic microphone response then the function generator voltage.

5.5.1 Setup

The setup shown in Figure 5.3 will be used for this test.

5.5.2 Method

Procedure

1. Set the function generator to the desired frequency and the lowest amplitude step.
2. Disconnect the PC speaker so there is no tone. Allow the lock-in amplifier to

lock to the signal and record the amplitude once it has settled. This is the measurement for 0V signal to the speaker.

3. Connect the speaker and record the amplitude once it has settled.

4. Increment the function generator voltage and record the amplitude once it has settled.

5. Repeat the previous step until the all voltage steps have been tested.

6. Change the frequency to the next selection and repeat the test until all frequencies have been tested.

The test will be repeated three times for each frequency, and the results averaged.

Test Parameters

Function Generator Voltage Range:	0 to 16V peak to peak
Voltage Step:	2V
Lock-In Time Constant:	10s
Settling Time:	40s
Laser Power:	0.5mW

The frequencies to be tested are: 500Hz, 1kHz, 2.5kHz, 5kHz, 10kHz, 15kHz and 20kHz .

5.5.3 Results

Table 5.2: Results of the fibre-optic microphone frequency test at 500Hz.

Function Generator (V)	Test 1 (dB)	Test 1 (μV)	Test 2 (dB)	Test 2 (μV)	Test 3 (dB)	Test 3 (μV)
0	64.5	0	62.7	0	63.5	0
2	68.9	20	68.4	30	68.9	50
4	73.5	30	73.3	30	73.7	40
6	76.4	40	76.1	100	76.5	110
8	78.5	40	78.6	120	78.7	130
10	80.3	70	80.3	120	80.3	170
12	81.8	140	82.4	170	82.3	160
14	83.5	170	83.1	180	83.2	14
16	84.4	300	84.4	210	84.7	330

Table 5.3: Averaged results of the fibre-optic microphone frequency test at 500Hz.

Function Generator (V)	Average Sound Level (dB)	Average Response (μV)
0	63.57	0.00
2	68.73	33.33
4	73.50	33.33
6	76.33	83.33
8	78.60	96.67
10	80.30	120.00
12	82.17	156.67
14	83.27	121.33
16	84.50	280.00

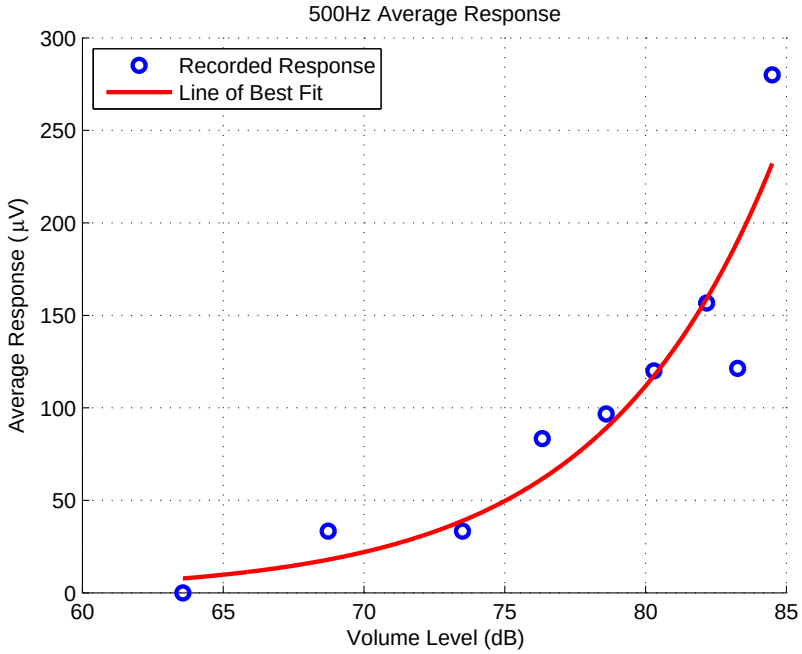

Figure 5.5: A plot of the results of frequency testing at 500Hz, including data points and an exponential curve fit to the data.

Table 5.4: Results of the fibre-optic microphone frequency test at 1kHz.

Function Generator (V)	Test 1 (dB)	Test 1 (μV)	Test 2 (dB)	Test 2 (μV)	Test 3 (dB)	Test 3 (μV)
0	65	0	64.7	0	64.99	0
2	74.5	40	74.5	10	74	10
4	80.2	30	80.9	30	80.2	30
6	83.6	60	83.8	40	83.7	60
8	86.1	90	86.1	50	86.3	80
10	87.7	110	88	70	88.3	60
12	89.5	120	89.8	120	89.9	100
14	90.9	150	91	130	91.3	170
16	92	180	92.2	210	92.5	190

Table 5.5: Averaged results of the fibre-optic microphone frequency test at 1kHz.

Function Generator (V)	Average Sound Level (dB)	Average Response (μV)
0	64.90	0.00
2	74.33	20.00
4	80.43	30.00
6	83.70	53.33
8	86.17	73.33
10	88.00	80.00
12	89.73	113.33
14	91.07	150.00
16	92.23	193.33

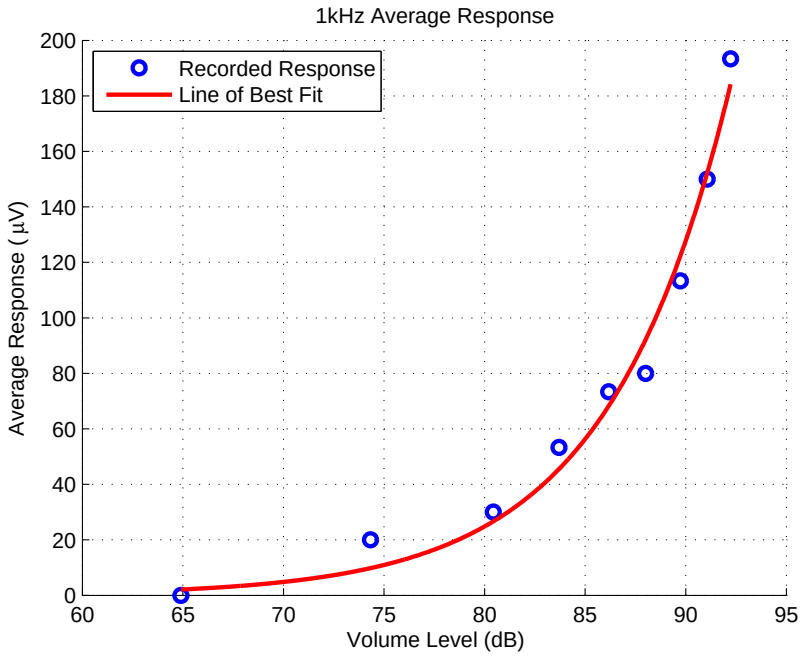

Figure 5.6: A plot of the results of frequency testing at 1kHz, including data points and an exponential curve fit to the data.

Table 5.6: Results of the fibre-optic microphone frequency test at 2.5kHz.

Function Generator (V)	Test 1 (dB)	Test 1 (μV)	Test 2 (dB)	Test 2 (μV)	Test 3 (dB)	Test 3 (μV)
0	65	0	65.4	0	64.5	0
2	70	0	69.9	10	70.2	0
4	74.4	0	75	0	75.1	10
6	77.9	20	78	10	78.3	20
8	80	20	80.2	10	80.5	20
10	82.2	30	82.4	20	82.4	20
12	83.7	20	83.8	30	83.8	30
14	85.1	40	85.2	30	85.2	40
16	86.5	50	86.6	50	86.7	40

Table 5.7: Averaged results of the fibre-optic microphone frequency test at 2.5kHz.

Function Generator (V)	Average Sound Level (dB)	Average Response (μV)
0	64.97	0.00
2	70.03	3.33
4	74.83	3.33
6	78.07	16.67
8	80.23	16.67
10	82.33	23.33
12	83.77	26.67
14	85.17	36.67
16	86.60	46.67

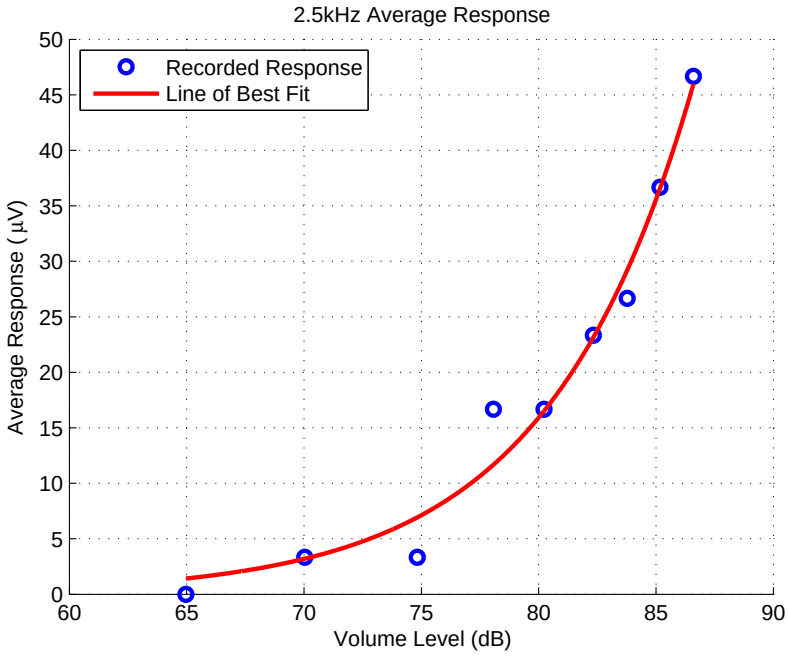

Figure 5.7: A plot of the results of frequency testing at 2.5kHz, including data points and an exponential curve fit to the data.

Table 5.8: Results of the fibre-optic microphone frequency test at 5kHz.

Function Generator (V)	Test 1 (dB)	Test 1 (μV)	Test 2 (dB)	Test 2 (μV)	Test 3 (dB)	Test 3 (μV)
0	64.6	0	65.2	0	64.7	0
2	69.2	30	69.3	10	68.9	0
4	73.4	10	73.3	20	73.7	10
6	77.2	30	78	40	77.6	10
8	79.4	70	79.5	50	79.4	60
10	82.5	80	82	100	82.6	60
12	86.4	120	86.2	140	86.6	120
14	87.8	160	87.5	110	88	140
16	89.1	190	89	200	89.4	180

Table 5.9: Averaged results of the fibre-optic microphone frequency test at 5kHz.

Function Generator (V)	Average Sound Level (dB)	Average Response (μV)
0	64.83	0.00
2	69.13	13.33
4	73.47	13.33
6	77.60	26.67
8	79.43	60.00
10	82.37	80.00
12	86.40	126.67
14	87.77	136.67
16	89.17	190.00

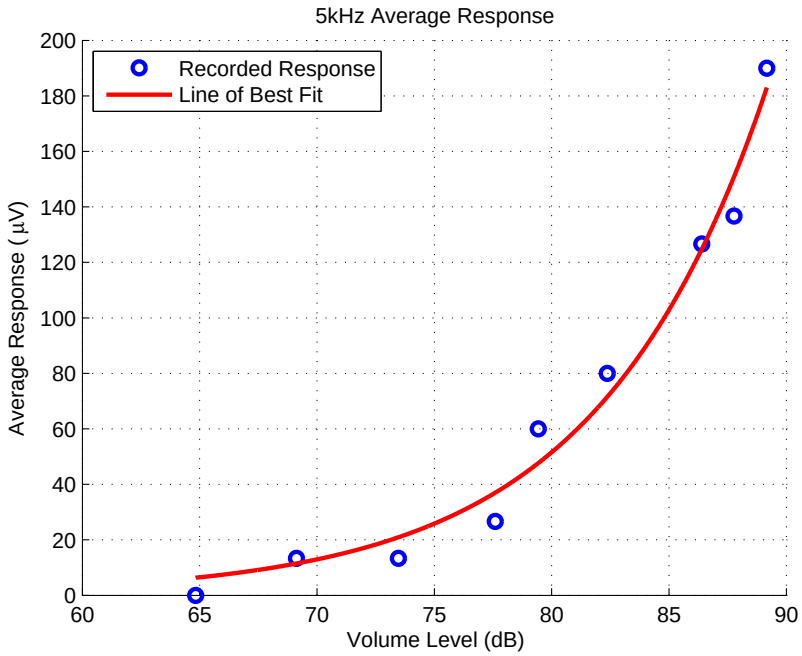

Figure 5.8: A plot of the results of frequency testing at 5kHz, including data points and an exponential curve fit to the data.

Table 5.10: Results of the fibre-optic microphone frequency test at 10kHz.

Function Generator (V)	Test 1 (dB)	Test 1 (μV)	Test 2 (dB)	Test 2 (μV)	Test 3 (dB)	Test 3 (μV)
0	64.2	0	64.7	0	63.7	0
2	67.2	10	71.5	20	71.1	30
4	71.2	20	76.1	30	76.3	30
6	75.5	30	79.4	60	79.4	50
8	79.4	50	81.1	70	81.9	70
10	81.7	70	83.7	80	83.6	60
12	85.5	130	85.1	160	84.9	170
14	86.2	140	86.8	180	86.3	160
16	87.4	220	88.1	210	87.5	170

Table 5.11: Averaged results of the fibre-optic microphone frequency test at 10kHz.

Function Generator (V)	Average Sound Level (dB)	Average Response (μV)
0	64.20	0.00
2	69.93	20.00
4	74.53	26.67
6	78.10	46.67
8	80.80	63.33
10	83.00	70.00
12	85.17	153.33
14	86.43	160.00
16	87.67	200.00

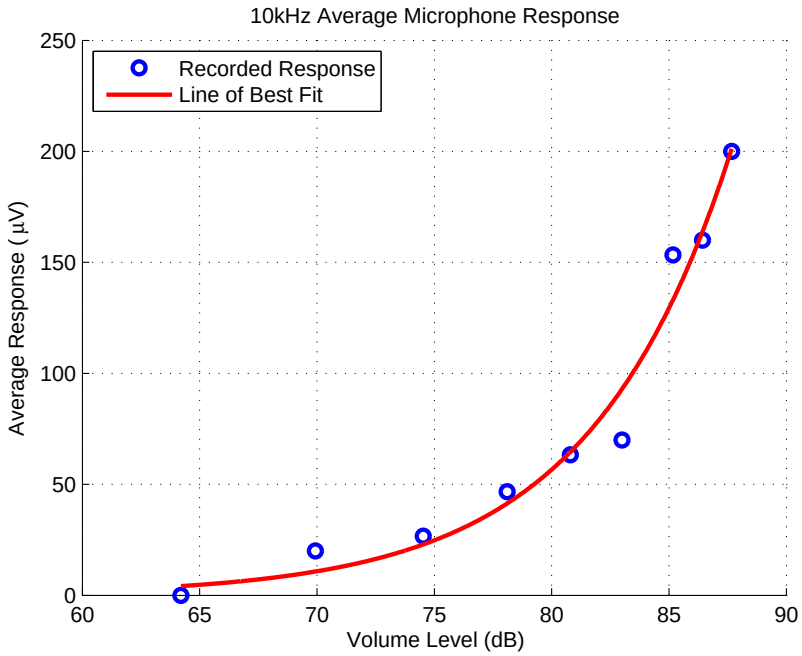

Figure 5.9: A plot of the results of frequency testing at 10kHz, including data points and an exponential curve fit to the data.

Table 5.12: Results of the fibre-optic microphone frequency test at 15kHz.

Function Generator (V)	Test 1 (dB)	Test 1 (μV)	Test 2 (dB)	Test 2 (μV)	Test 3 (dB)	Test 3 (μV)
0	65.1	0	65.8	0	65.2	0
2	73	40	72.9	10	72.7	0
4	77.7	60	77.5	10	78	30
6	81.2	130	81.4	30	81.2	20
8	83.8	80	83.5	100	83.8	110
10	86.4	100	85.9	100	85.8	120
12	86.8	210	87.2	260	87.5	160
14	88.4	250	88.6	180	88.6	210
16	90.4	360	89.5	200	89.7	210

Table 5.13: Averaged results of the fibre-optic microphone frequency test at 15kHz.

Function Generator (V)	Average Sound Level (dB)	Average Response (μV)
0	65.37	0.00
2	72.87	16.67
4	77.73	33.33
6	81.27	60.00
8	83.70	80.00
10	86.03	100.00
12	87.17	190.00
14	88.53	213.33
16	89.87	256.67

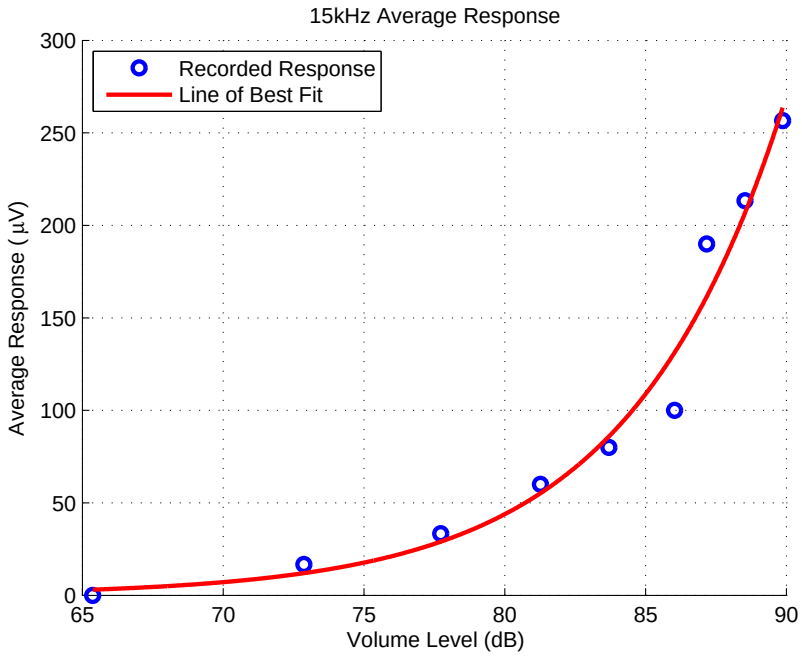

Figure 5.10: A plot of the results of frequency testing at 15kHz, including data points and an exponential curve fit to the data.

Table 5.14: Results of the fibre-optic microphone frequency test at 20kHz.

Function Generator (V)	Test 1 (dB)	Test 1 (μV)	Test 2 (dB)	Test 2 (μV)	Test 3 (dB)	Test 3 (μV)
0	63.6	0	65.4	0	64.5	0
2	65.8	0.04	66.5	0.01	66	0.01
4	69.5	0.04	68.5	0.04	70	0.02
6	71.1	0.06	69.9	0.06	71.6	0.05
8	74.3	0.12	74.2	0.11	74.5	0.1
10	74.6	0.13	76.2	0.12	75.8	0.12
12	77	0.15	77.4	0.1	77.1	0.15
14	78.1	0.15	78.7	0.15	77.8	0.14
16	78.8	0.16	79.3	0.26	79	0.18

Table 5.15: Averaged results of the fibre-optic microphone frequency test at 20kHz.

Function Generator (V)	Average Sound Level (dB)	Average Response (μV)
0	64.50	0.00
2	66.10	20.00
4	69.33	33.33
6	70.87	56.67
8	74.33	110.00
10	75.53	123.33
12	77.17	133.33
14	78.20	146.67
16	79.03	200.00

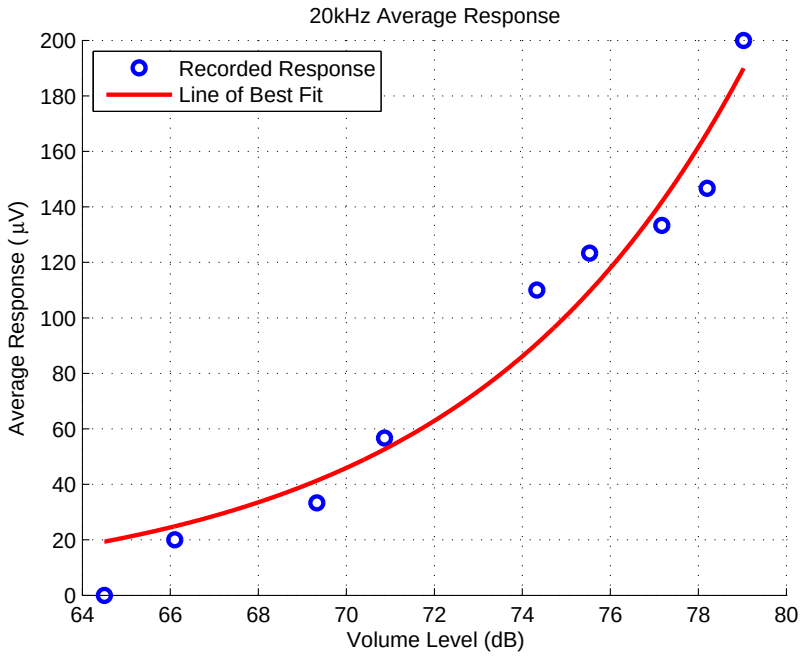

Figure 5.11: A plot of the results of frequency testing at 20kHz, including data points and an exponential curve fit to the data.

Frequency Response Comparison

Figure 5.12 shows a comparison of the microphone response for each frequency selection.

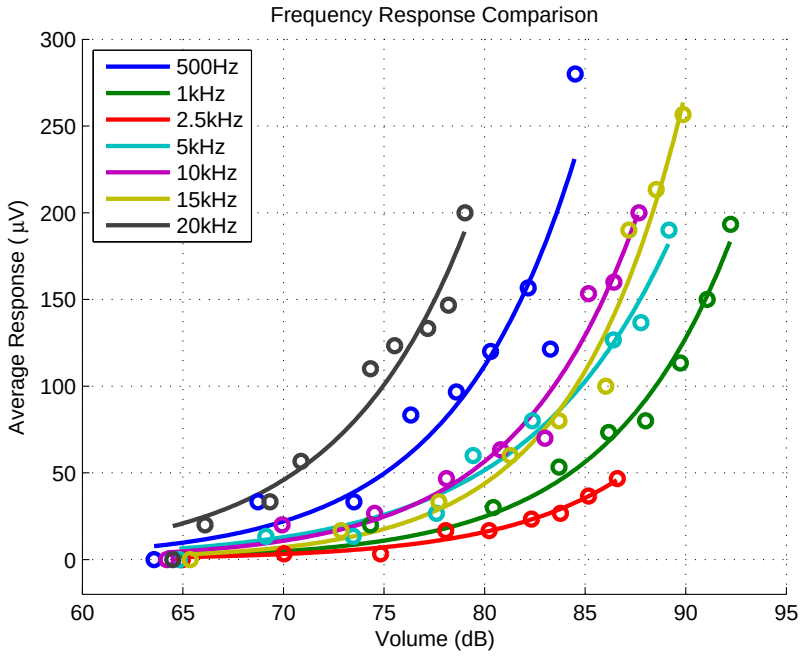

Figure 5.12: A plot showing the results of each frequency test on a single plot including data points, and an exponential curve fit to each data set.

5.5.4 Discussion

Figure 5.12 is useful for analysing how the microphone responds relative to frequency. This graph indicates that the fibre-optic microphone response was greater in amplitude at certain frequencies. There is however, no clear trend. That is, the overall response is not greater at higher frequencies nor vice versa.

The variation in response with frequency may be affected by resonance. In Section 4.5, the fundamental resonant frequency was calculated to be 1715Hz. This could play a role in the greater response at 20kHz and the lesser response at 2.5kHz as the 12th harmonic resonant frequency is quite close to 20kHz, while 2.5kHz is almost directly in between the first and second harmonic where a dull response would be expected. However, this does not explain the greater response at 500Hz, as this is well below the fundamental resonant frequency.

The frequency response exhibited here could also be a result of the sound reflecting

off and interacting with the bench top and other furniture in the lab. This too would be expected to have a varying impact on the response of the fibre-optic microphone at different frequencies.

Alternatively, the change in amplitude could be caused by the unavoidable time gap in between data collection. In this case, it could indicate a poor stability in the fibre-optic microphone response over time. This would be caused by variation in temperature in both the equipment, and in the room, as well as other environmental changes throughout the day.

5.5.5 Setup

The setup shown in Figure 5.3 will be used for this test.

5.6 Laser Power Level

The laser power setting will be adjusted in order to determine its effect on the microphone response. For each setting the response of the microphone, and the sound level will be measured as the volume of the tone is stepped up.

5.6.1 Method

Procedure

1. Set the function generator to the desired frequency and the lowest amplitude step.
2. Disconnect the PC speaker so there is no tone. Allow the lock-in amplifier to lock to the signal and record the amplitude once it has settled. This is the measurement for 0V signal to the speaker.
3. Connect the speaker and record the amplitude once it has settled.
4. Increment the function generator voltage and record the amplitude once it has settled.
5. Repeat the previous step until the all voltage steps have been tested.

6. Change the power level setting on the bench top laser and repeat until all selected settings have been tested.

Test Parameters

Function Generator Frequency:	1kHz
Function Generator Voltage Range:	0 to 16V peak to peak
Voltage Step:	2V
Lock-In Time Constant:	10s
Settling Time:	40s

The power settings to be tested are: 0.05mW, 0.1mW, 0.2mW, 0.3mW, 0.5mW, 0.7mW and 0.9mW.

5.6.2 Results

Table 5.16: Results of power level testing at 0mW.

Function Generator	Volume (dB)	Output (mV)
0	65.2	0
2	74.4	0
4	78.6	0
6	81.6	0
8	84.1	0
10	86.2	0
12	87.9	0
14	89	0
16	90.5	0

Table 5.17: Results of power level testing at 0.05mW.

Function Generator	Volume (dB)	Output (mV)
0	65.9	0
2	71.2	0
4	76.1	0
6	78.8	0
8	81.5	0
10	83.2	0
12	84.7	0
14	86.1	0
16	87.4	0

Table 5.18: Results of power level testing at 0.1mW.

Function Generator	Volume (dB)	Output (mV)
0	65.1	0
2	70.6	0
4	75.3	0
6	78.4	0
8	81.5	0
10	83.8	0
12	85.5	10
14	86.5	10
16	87.1	20

Table 5.19: Results of power level testing at 0.2mW.

Function Generator	Volume (dB)	Output (mV)
0	65.1	0
2	70.9	0
4	76.3	10
6	79.8	20
8	82.2	10
10	84.1	50
12	85.2	50
14	86.7	50
16	87.7	50

Table 5.20: Results of power level testing at 0.3mW.

Function Generator	Volume (dB)	Output (mV)
0	64.8	0
2	71.5	0
4	76.2	0
6	79.5	20
8	81.8	20
10	83.7	60
12	85.3	60
14	86.5	60
16	87.4	70

Table 5.21: Results of power level testing at 0.5mW.

Function Generator	Volume (dB)	Output (mV)
0	65.2	0
2	71.3	20
4	76.5	40
6	79.5	30
8	82.1	70
10	83.9	90
12	85.5	170
14	86.7	150
16	87.7	210

Table 5.22: Results of power level testing at 0.7mW.

Function Generator	Volume (dB)	Output (mV)
0	65	0
2	71.3	20
4	76.5	30
6	79.6	120
8	81.7	80
10	83.9	150
12	85.5	200
14	86.8	260
16	88.1	290

Table 5.23: Results of power level testing at 0.9mW.

Function Generator	Volume (dB)	Output (mV)
0	65.2	0
2	70.6	20
4	75.9	20
6	78.9	130
8	81.5	150
10	83.3	160
12	84.9	320
14	86.2	400
16	87.3	450

Power Level Comparison

Figure 5.13 shows the microphone responses at each power level plot on the same axis.

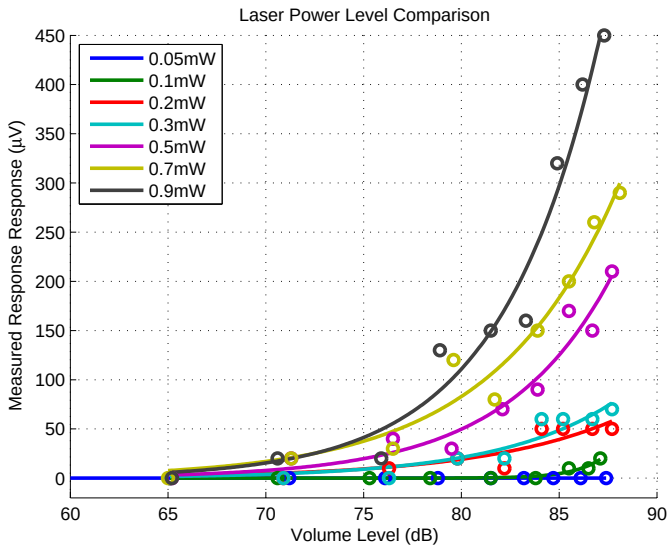

Figure 5.13: A plot showing the results of each power level test on a single plot including data points and an exponential curve fit to each data set.

5.6.3 Discussion

Figure 5.13 shows that as the power level is increased, the overall response of the fibre-optic microphone is increased. From this graph and the tabulated results, it is clear that for this system, 0.1mW of power is the minimum required to detect the audio signal. However, 0.5mW is a more appropriate setting, as it allows greater discrimination, and the detection of lower volume tones.

Increasing the power at the bench top laser will increase the output of photodetector, but this is a DC increase and does not directly affect in the lock-in amplifier measurement. However, the power is evenly divided between the sensing arm and reference arm, so greater power at the input of the interferometer results in greater power in each arm. If a changing phase delay occurs, the recombined signal will show interference which cycles between constructive and destructive. This interference will cause the amplitude to vary and the amplitude of this variation will be relative to the amplitude of the signal itself. So greater power from the source results in a higher amplitude interference resulting in a greater signal which is picked up by the lock-in amplifier.

It may seem obvious that disabling the laser, which is a power level of 0mW, would result in no output. However, this provides valuable insight into the operation of the fibre-optic microphone. Because the the signal picked up by the lock-in amplifier is so small, it is conceivable that the signal is being transferred to the lock-in amplifier by unintentional means. For instance, it is possible that the speaker could electromagnetically couple with the leads on the input of the lock-in amplifier and hence transfer the signal this way. However, because there is no output while the laser is disabled, this possibility can be ruled out, hence confirming the fibre-optic microphone functions as designed.

5.7 Carrier Signal Test

It is possible to modulate the bench top laser with a signal from the function generator. If this signal is also used as the reference for the lock-in amplifier, it can act as a carrier for the microphone. While using a carrier signal, the response of the microphone, as well as the sound level will be recorded as the tone volume is stepped.

5.7.1 Setup

The setup for carrier test will be different to the previous tests. Figure 5.14 shows the set up used to perform the carrier signal test. The second channel on the function generator is now being used to modulate the laser to provide a carrier signal. This channel is also used as the reference input on the lock-in amplifier. The first channel on the function generator is still used to feed the speaker so that the carrier frequency and tone frequency can be set independently.

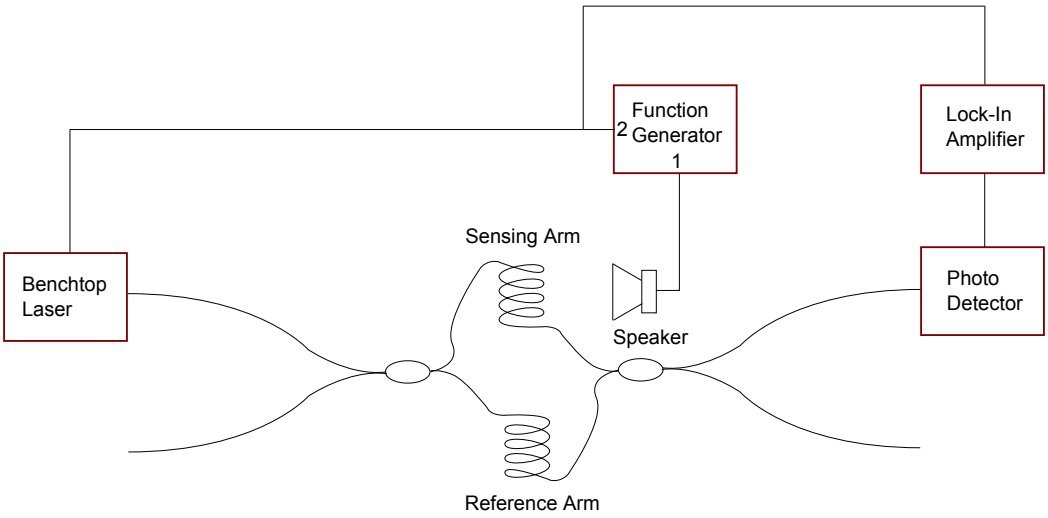

Figure 5.14: A diagram shown the experiment set up used for the carrier frequency test (Source: Author).

5.7.2 Method

Procedure

1. Connect channel 2 on the function generator to the modulation input of the bench top laser, and set it to the desired carrier frequency.

2. Set channel 1 on the function generator (connected to speaker) to the desired frequency and and the lowest amplitude step.

3. Disconnect the PC speaker so there is no tone. Allow the lock-in amplifier to lock to the signal and record the amplitude once it has settled. This is the measurement for 0V signal to the speaker.

4. Connect the speaker and record the amplitude once it has settled.

5. Increment the function generator voltage and record the amplitude once it has settled.

6. Repeat the previous step until the all voltage steps have been tested.

7. Change the carrier frequency and tone frequency as required, and repeat the test until each specified setting has been trialled.

Test Parameters

Carrier Frequency:	1kHz and 1.5kHz
Carrier Offset	1.5V
Carrier Amplitude	3V peak to peak
Tone Frequency:	1kHz and 1.5kHz
Function Generator Voltage Range:	0 to 16V peak to peak
Voltage Step:	2V
Lock-In Time Constant:	10s
Settling Time:	40s
Laser Power:	0.5mW (modulated)

5.7.3 Results

Table 5.24: Results of carrier test using a 1.5kHz carrier signal and a 1kHz tone.

Function Generator	Volume (dB)	Output (mV)
0	65.1	18.26
2	73.4	17.61
4	79.4	19.32
6	82.4	17.27
8	85.8	15.42
10	87.1	19.24
12	88.8	18.97
14	89.4	19.46
16	91	15.42

Table 5.25: Results of carrier test using a 1.5kHz carrier signal and a 1.5kHz tone

Function Generator	Volume (dB)	Output (mV)
0	65.3	23.1
2	73.1	12.68
4	78.5	24.67
6	82.1	17.73
8	85	20.99
10	87.9	9.09
12	88.6	12.22
14	90	8.75
16	90.9	12.52

Table 5.26: Results of carrier test using a 1kHz carrier signal and a 1kHz tone

Function Generator	Volume (dB)	Output (mV)
0	64.8	15.85
2	73.3	12.65
4	77.8	14.68
6	82	8.72
8	84.9	14.34
10	87.8	16.71
12	88.7	23.31
14	89.8	15.89
16	91	12.01

Table 5.27: Results of carrier test using a 1kHz carrier and a 1.5kHz tone

Function Generator	Volume (dB)	Output (mV)
0	65.2	14.57
2	73.2	16.89
4	77.8	21.77
6	82.1	12.08
8	84.8	8.86
10	87.5	9.91
12	89.1	12.12
14	90.6	8.81
16	91.4	15.46

5.7.4 Discussion

The results of this test show that the use of a carrier signal is not feasible. When a carrier signal is used, the lock-in amplifier will not settle to 0mV whether a tone is present or not. Furthermore, the amplitude of the lock-in amplifier reading does not increase proportionally with the volume of the tone, instead, it varies unpredictably in either direction. Because of this, there is no means of differentiating when a tone is present, and when it is not. Neither does the measurement give any indication of the volume of the tone.

Because the carrier signal is always present, the lock-in amplifier will not settle to zero when the audio tone is not present. When the lock-in amplifier was locked to the tone frequency as in all previous testing, influences such as fluctuating temperature, interference from light and unrelated sound are all ignored. When the lock-in amplifier is instead locked to a carrier frequency, its output is sensitive to these noise sources and the output amplitude drifts. Finally, the period of the audio tone is always much less than the integrating time constant used on the lock-in amplifier. This means, after integration, the influence of the tone is cancelled out. Because of this, lock-in amplifier measurements are seemingly random, and do not correspond to the volume of the tone.

5.8 Evaluation

Initial testing aimed to prove the the fibre-optic microphone is functional. Figure 5.4 shows that the microphone response read from the lock-in amplifier is proportional to the volume of an audio tone at the locked frequency. Specifically, it shows exponential proportionality which would need to be accounted for in practical use. This shows that the fibre-optic microphone is functional and is fit for use in photoacoustic spectroscopy.

The fibre-optic microphone was tested over a range of frequencies and a comparison of the response at each frequency tested is shown in Figure 5.12. This shows variation in the overall amplitude between the difference frequencies tested. The results do not however indicate a clear trend in the frequency response of the fibre-optic microphone. That is, the response amplitude does not increase with frequency or vice versa. This may be a result of resonance, and the acoustic waves interacting with the desk and

other surrounding furniture in the labs. It may otherwise indicate a lack of stability over time, meaning that the response of the fibre-optic microphone varies throughout the day due to temperature changes and other such factors. Further testing may be needed to determine the exact cause of the change in response with frequency, but the current results show that the fibre-optic microphone is function over the entire frequency tested.

The fibre-optic microphone was tested with different power level settings on the benchtop laser. The results of this testing in Figure 5.13 show that the fibre-optic microphone response is directly affected by the power level of the benchtop laser. A greater power level results in a greater response. The minimum setting for this configuration is roughly 0.5mW depending on the application.

The final test explored the possibility of introducing a carrier frequency by modulating the benchtop laser with a signal which the lock-in amplifier is locked to. The numeric result of this test show no relation between volume received and the response at the lock-in amplifier. This mode of operation can be considered unsuccessful and not recommended for implementation.

In summation, the fibre-optic microphone was found to be functional. The output of the fibre-optic microphone in the lock-in amplifier measurement was found to be exponentially proportional to the volume of a tone at the locked frequency. Overlooking the variation in response at different frequencies, the fibre-optic microphone was functional over the entire range tested. The power level of the laser was found to directly affect the fibre-optic microphones output amplitude, requiring a minimum of approximately 0.5mW. The use of a carrier signal in the fibre-optic microphone was unsuccessful. Despite this, the concept of the fibre-optic microphone was proven, and a functioning prototype has been created.

Chapter 6

Conclusions and Further Work

This chapter concludes the dissertation. The project objects will be addressed, discussing how each was or was not achieved. Within the area of the project topic, there is much work yet to be done. This includes further testing, improving the design and trialling other fibre-optic microphone designs. Further work in this area will be discussed in this chapter. Finally, the conclusion will be given. This will be a short review of the major achievements and observations of the project.

6.1 Achievement of Project Objectives

Please refer to Appendix A for the Project Specification containing the project objectives.

The project specification defines eight objectives. Objectives 1 to 5 are the main objectives of the project, and each of these has been achieved. Objectives 6 to 8 were to be completed as time permits. Of these, objectives 6 and 7 were achieved.

Objective 1 involves the research of the major concepts of the project including fibre-optic sensors and how they are used in microphone applications. This theory has been researched, and covered in Chapters 1 to 3.

Objective 2 requires investigation of the current work in the area of fibre-optic microphones. This investigation was conducted, and several examples of previously successful

fibre-optic microphones are given in Chapter 3.

Objective 3 is the main object of this project. It requires the design of a fibre-optic microphone based on the literature. This design was proposed in Chapter 4.

Objective 4 focuses on preparations in order to construct and test the microphone. This is both gathering the equipment and preparing safety documentation. All necessary equipment was provided by USQ. Chapter 4 gives an overview of the equipment used. The safety documentation has been provided in Appendix B.

Objective 5 is to construct and test the fibre-optic microphone. The fibre-optic microphone was constructed as designed, and the results of testing are shown in Chapter 5.

Objective 6 is to incorporate the lock-in amplifier. The lock-in amplifier is included in the design and is a necessary piece of equipment as the signal received by the microphone is so small, that it would be otherwise difficult to detect.

Objective 7 is to explore and discuss methods of improving the microphone beyond the original design. These methods have been discusses in Chapter 6 in the Further Work section.

Objective 8 requires the implementation of the improvement methods mentioned in objective 7. Unfortunately due to time restraints, none of these improvements were trialled.

6.2 Further Work

6.2.1 Improving Stability

Observing the output of the microphone at the output of the photodetector on an oscilloscope reveals lacking stability. This output shows frequently DC drift caused by background noise and cross sensitivity to temperature and light. For the most part this does not interfere with the reading as it is ignored by the lock-in amplifier. It would be beneficial to reduce this DC drift in order to make the system more stable overall, and allow exploration of extracting the output by means other than the lock-in amplifier

such as Fourier analysis.

The coupler used in constructing the microphone has a very thin jacket on each lead, only 900μm in diameter. This aids in allowing sound to modulate the sensing arm. However, because the reference arm has a jacket of the same thickness, it too is sensitive to sound. It also leaves the entire length of the coupler more exposed to light and temperature. Couplers are available which have a thicker jacket or no lead exiting the coupler joint. An example of this type of coupler is shown in Figure 6.1. With this type of coupler, the sensing arm could be constructed from a lead with a thin jacket while the reference arm could be constructed from a patch lead of equal length, but with a thick jacket. This could decrease interference without decreasing sensitivity though care would need to be taken to ensure that the reference and sensing arms are equal in length to a precise degree otherwise an initial phase difference between the two would be introduced.

Figure 6.1: An image of a Thorlabs 1x4 coupler with a thicker jacket which could be used to reduce noise in the fibre-optic microphone. A similar 2x2 50/50 coupler would be ideal (Source: Thorlabs FCQ1315 1x4 Coupler).

6.2.2 Increasing Sensitivity

It is likely that the volume of the tone produced in photoacoustic spectroscopy would be less than that used to test the microphone. Because of this, it would be necessary to increase the sensitivity of the device before using it in such an application.

The lock-in amplifier was set to 100mV for all tests. It is capable of sensitivities much lower than this. However, while on these settings, the amplitude measurement while proportional to the volume of the tone, was unstable and did not settle. Because of this, taking readings would be inaccurate. If the stability of the device was improved as suggested in the previous section, it may enable the use of more sensitive settings.

This would then enable the microphone to pick up lower volume tones with greater discrimination.

Experimentation with the sensor head could also lead to increased sensitivity. Attaching the sensing arm of the interferometer fibre to the PVC former with a bond stronger than duct tape, for instance epoxy or a strong glue, could lead to better transferral of vibration between the two. Alternatively, an entirely different sensor head design could be implemented. For example, attaching the sensing fibre to some form of membrane constructed from a film stretched tightly across a former could be trialled.

In testing, it was found the fire-optic microphone response would vary with frequency. It was discussed that this could be an effect of resonance, but this was unable to be confirmed. Further testing could reveal what role resonance and other factors play in the response of the fibre-optic microphone at different frequencies. Doing so could enable this effect to be exploited by matching the audio frequency used to the resonant frequency of the sensor head or vice versa. This would result in resonance in the sensor head and may provide a greater amplitude response from the fibre-optic microphone.

6.2.3 Implementable Design

The design constructed for the project is mainly experimental. The equipment used is expensive and would most likely not be cost effective to implement in a practical situation. There are several ways in which the overall cost could be reduced.

The Thorlabs S1FC bench top laser which was used is very good for testing the device. It provided the facility to modulate the laser source and set the power level. However, modulation of the laser source did not prove to be successful, and in a practical scenario, the ability to adjust the power level would likely be unnecessary. This laser is also capable of higher power levels than required as it was found that only 0.5mW was necessary for operation. Replacing this laser with a simpler, lower powered laser would reduced the cost of this component significantly.

The Thorlabs PDA8GS Photodetector used is also a higher quality detector than would be required by a practical system. A cheaper fibre coupled photo diode could be purchased or designed using cheaper components.

6.2.4 Trial Alternate Designs

The decision was made to base the design of the microphone on a Mach-Zehnder interferometer. This decision was based on literature which indicated that this design would be simpler and more sensitive than a design based on a Michelson or Sagnac interferometer. These designs could be constructed and tested to confirm that the Mach-Zehnder based design is indeed more sensitive. This would however require the acquisition of further components.

The Fabry-Perot interferometer was also investigated as a design option. The Mach-Zehnder configuration was chosen over the Fabry-Perot mainly due to the complication of constructing a Fabry-Perot based design. In fact the literature indicated that a well constructed Fabry-Perot interferometer based design would be likely to be more sensitive than the Mach-Zehnder. If the equipment were available, a design based on the Fabry-Perot interferometer could be trialled.

6.3 Conclusions

Research into the theory behind fibre-optic microphones was conducted, incorporating the basics of fibre-optics and fibre-optic sensors as well as interferometry. This background theory is discussed in Chapter 2 . In addition to this, the concepts of photoacoustic spectroscopy and lock-in amplifiers was researched and covered in Chapter 3.

This background information enabled a fibre-optic microphone design to be developed. Chapter 4 proposes this design and shows that the Mach-Zehnder interferometer is the interferometer best suited to the fibre-optic microphone.

The design was successfully implemented and testing was performed in order to determine if the microphone was functioning as planned. The results of this testing are shown in Chapter 5.

This testing revealed that the microphone was functional and that the microphone produced a response proportional to the volume of the tone it received. Testing was performed over a range of audio frequencies. This range was limited by that which the

speaker was capable of, but the microphone was capable of operation for this entire range.

There was some fluctuation in overall response at different frequencies, but with no clear relationship between the response amplitude and tone frequency. It is likely that resonance of the sensor head played a role in the frequency response of the fibre-optic microphone, but this was not shown conclusively. Further testing would be needed to investigate this possibility.

Testing showed that the power level of the laser was directly linked to the amplitude response of the microphone with lower power levels resulting in less discrimination at the lower volumes. Because of this, the minimum power level required for operation of the fibre-optic microphone is approximately 0.5mW. The microphone was also tested with the laser disabled in order to rule out the possibility that speaker was electromagnetically coupled with the lock-in amplifier leads. There was no signal detected with the laser disabled, indicating that there was no electromagnetic coupling, and that the microphone was operating as designed.

Testing was also carried out to determine if the use of a carrier frequency (via modulation of the laser) was a viable mode of operation for the microphone. This did not prove to be viable as the lock-in amplifier reading for any given input would fluctuate and and would not settle. Due to this the output is unrelated to the tone, and useful in determining its volume.

In summation, the testing showed successful operation of fibre-optic microphone and proof of this concept. Improvements to the fibre-optic microphone have been proposed, but were unable to be implemented due to time constraints. Excluding the implementation of these design improvements, the objectives of the project were achieved. A working fibre-optic microphone was developed and shown to be fit for its application in photoacousic spectroscopy.

References

AMETEK Model 7270 DSP Lock-in Amplifier Instruction Manual (2010).

Baird, R. (1967), 'RF Measurements of the Speed of Light', *Proceedings of the IEEE* **55**(6), 1032–1039.

Ball, D. W. (2006), 'The Baseline Photoacoustic Spectroscopy. (cover story).', *Spectroscopy* **21**(9), 14 – 16.

Banuelos-Saucedo, M. & Ozanyan, K. (2012), Fast Response Lock-In Amplifier, *in* 'Instrumentation and Control Technology (ISICT), 2012 8th IEEE International Symposium on', pp. 122–125.

Breguet, J., Pellaux, J. & Gisin, N. (1995), 'Photoacoustic Detection of Trace Gases with an Optical Microphone', *Sensors and Actuators A: Physical* **48**(1), 29 – 35.

Byeong Ha, L., Young Ho, K., Kwan Seob, P., Joo Beom, E., Myoung Jin, K., Byung Sup, R. & Hae Young, C. (2012), 'Interferometric Fiber Optic Sensors.', *Sensors (14248220)* **12**(3), 2467 – 2486.

Crisp, J. (1996), *Introduction to Fiber Optics*, Newnes.

Culshaw, B. (1984), *Optical Fibre Sensing and Signal Processing*, P. Peregrinus on behalf of the Institution of Electrical Engineers.

Culshaw, B. (2006), 'The Optical Fibre Sagnac Interferometer: an Overview of its Principles and Applications', *Measurement Science and Technology* **17**(1), R1.

Dakin, J. & Culshaw, B. (1988), *Optical Fiber Sensors: Principles and Components*, Artech House telecommunications library, Artech House.

Dyson, J. (1970), *Interferometry as a Measuring Tool*, Machinery Publishing.

Ecke, W., Chen, K. & Jinsong, L. (2012), 'Fiber Optic Sensors.', *Journal of Sensors* p. 1.

Françon, M. (1966), *Optical Interferometry*, Academic Press.

Furstenau, N., Horack, H. & Schmidt, W. (1998), 'Extrinsic Fabry-Perot Interferometer Fiber-Optic Microphone', *Instrumentation and Measurement, IEEE Transactions on* **47**(1), 138–142.

Giancoli, D. (1991), *PHYSICS Third Edition*, Prentice Hall.

Grattan, K. & Sun, T. (2000), 'Fiber Optic Sensor Technology: an Overview', *Sensors and Actuators A: Physical* **82**(13), 40 – 61.

Haisch, C. & Niessner, R. (2002), 'Light and Sound - Photoacoustic spectroscopy', *spectrosc eur* **14**(5), 10–15.

Harren, F. J., Cotti, G., Oomens, J. & Hekkert, S. t. L. (2000), 'Photoacoustic Spectroscopy in Trace Gas Monitoring', *Encyclopedia of Analytical Chemistry* .

Kersey, A. D. (1996), 'A Review of Recent Developments in Fiber Optic Sensor Technology', *Optical Fiber Technology* **2**(3), 291 – 317.

Kruger, L. & Theron, H. (2007), Optical Fibre Mach-Zehnder Microphone, *in* 'Microwave and Optoelectronics Conference, 2007. IMOC 2007. SBMO/IEEE MTT-S International', pp. 389–391.

Kyriakou, K. & Fisher, H. R. (2013), 'Benefits of the fiber optic versus the electret microphone in voice amplification', *International Journal of Language & Communication Disorders* **48**(1), 115–126.

Lingenfelter, D. (2001), 'Fiber Optic Safety.', *Broadcast Engineering* **43**(7), 74.

Manual for Larson Davis SoundTrack LxT1 (2013).

Mayfield, J., Parham, R. & Webber, B. (1984), *Fundamentals of Senior Physics*, Fundamentals of Senior Physics, Heinemann Educational Australia.

NessAiver, M. S., Stone, M., Parthasarathy, V., Kahana, Y. & Paritsky, A. (2006), 'Recording high quality speech during tagged cine-mri studies using a fiber optic microphone', *Journal of Magnetic Resonance Imaging* **23**(1), 92–97.

Ohashi, C. (2010), Optical Fibers: History and Future Perspectives, *in* 'OptoeElectronics and Communications Conference (OECC), 2010 15th', pp. 34–35.

RIGOL DG4062 Function/Arbitrary Waveform Generator User Guide (2011).

Sadiku, M. (2010), *Elements of Electromagnetics*, Oxf Ser Elec Series, Oxford University Press, Incorporated.

Thorlabs 1 x 4 Single Mode Fiber Couplers (2013).

Thorlabs 2 x 2 Single Mode Fiber Couplers and Taps (2013).

Thorlabs PDA8GS Fibre Coupled Photodetector Specification Sheet (2010).

Thorlabs S1FC Fibre Coupled Laser Source Operating Manual (2013).

Yin, S., Ruffin, P. & Yu, F. (2010), *Fiber Optic Sensors, Second Edition*, Optical Science and Engineering, Taylor & Francis.

Appendix A

Project Specification

University of Southern Queensland

ENG4111\4112
Project Specification

FOR:	Isaac KENNEDY
TOPIC:	Design and Development of a Fibre-Optic Microphone
SUPERVISOR:	Dr John Leis
PROJECT AIM:	To devise through research a method of construction of a fibre-optic microphone with the final aim of designing and constructing a working system.

PROGRAMME: **Issue A, 18th March 2014**

1. Research the theory behind the use of fibre-optic sensors in microphone and sound detection applications.
2. Investigate current work in the area of fibre-optic sensors, and fibre-optic microphones.
3. Based on the literature, devise the most appropriate design taking into account the application and available equipment.
4. Gather and study the use of the required equipment while preparing the necessary safety documentation.
5. Construct and test the fibre-optic microphone.

As time permits:

6. Investigate the use of a single-frequency lock-in configuration, and if possible test this concept.
7. Explore and discuss how the construction maybe improved including enhanced sensitivity, and reduced size and use of materials.
8. Implement and test any possible improvements discovered.

Agreed: _____ _____ _____ _____

(Student) (Date) (Supervisor) (Date)

_____ _____

(Examiner) (Date)

Appendix B

Risk Management Plan

University of Southern Queensland

Generic Risk Management Plan

Workplace (Division/Faculty/Section): Faculty of Health, Engineering and Sciences		
Assessment No (if applicable):	Assessment Date: / /	Review Date: (5 years maximum) / /
Context: What is being assessed? Describe the item, job, process, work arrangement, event etc: Beng Project - Design and development of a fibre-optic microphone, involving working with low level laser and optical fibre.		
Assessment Team – who is conducting the assessment?		
Assessor(s): Dr. John Leis Others consulted: (eg elected health and safety representative, other personnel exposed to risks)		

The Risk Management Process

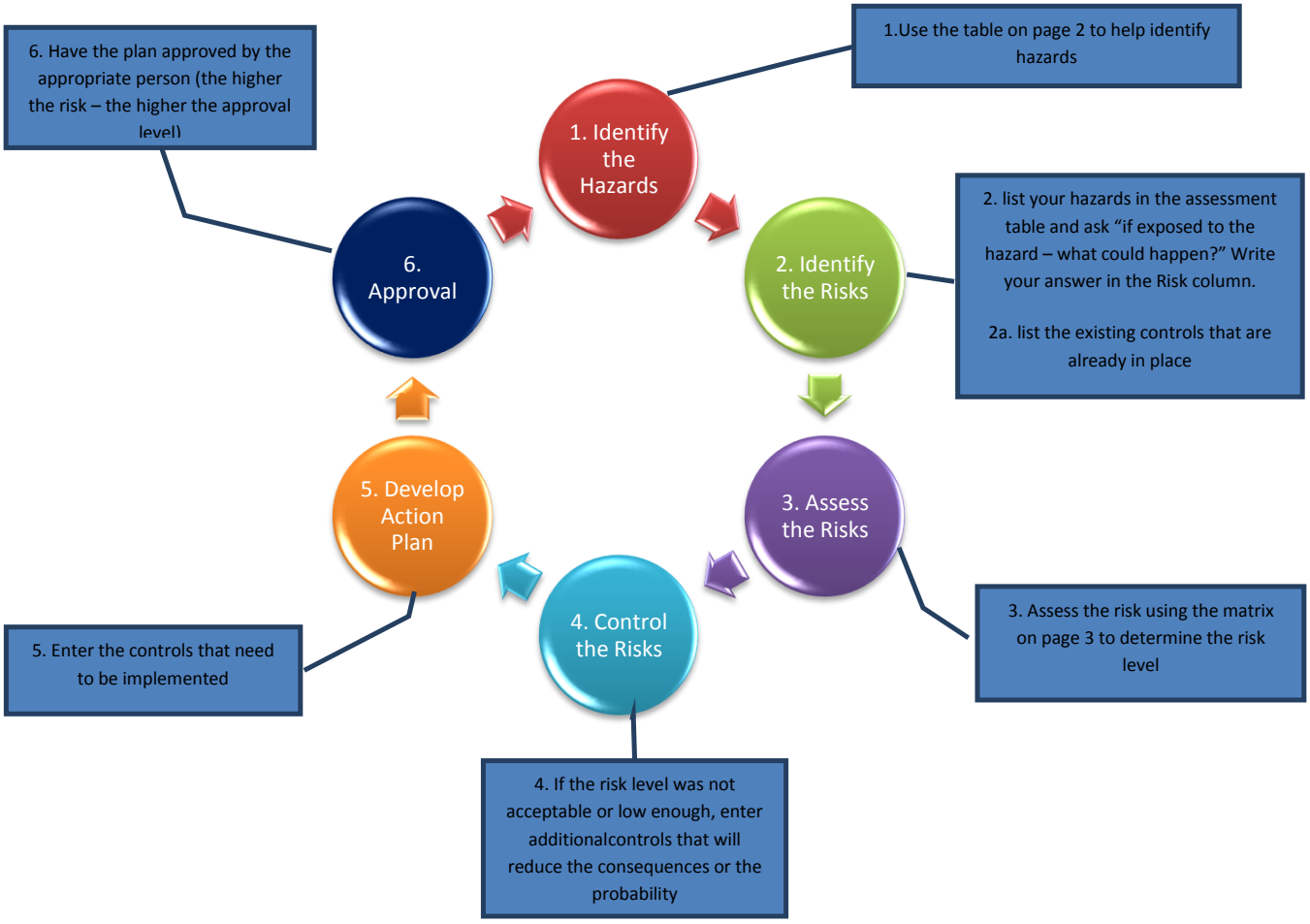

Step 1 - **Identify the hazards**(use this table to help identify hazards then list all hazards in the risk table)		
General Work Environment		
☐ Sun exposure	☐ Water (creek, river, beach, dam)	☐ Sound / Noise
☐ Animals / Insects	☐ Storms / Weather/Wind/Lightning	☐ Temperature (heat, cold)
☐ Air Quality	☐ Lighting	☐ Uneven Walking Surface
☐ Trip Hazards	☐ Confined Spaces	☐ Restricted access/egress
☐ Pressure (Diving/Altitude)	☐ Smoke	☐
Other/Details:		
Machinery, Plant and Equipment		
☐ Machinery (fixed plant)	☐ Machinery (portable)	☐ Hand tools
☐ Laser (Class 2 or above)	☐ Elevated work platforms	☐ Traffic Control
☐ Non-powered equipment	☐ Pressure Vessel	☒ Electrical
☐ Vibration	☐ Moving Parts	☐ Acoustic/Noise
☐ Vehicles	☐ Trailers	☐ Hand tools
Other/Details: Electrical - 240V mains supply - Thorlabs S1FC fibre couple laser soure. 12V DC - Thorlabs PDA8GS fibre coupled photodetector		
Manual Tasks / Ergonomics		
☐ Manual tasks (repetitive, heavy)	☐ Working at heights	☐ Restricted space
☐ Vibration	☐ Lifting Carrying	☐ Pushing/pulling
☐ Reaching/Overstretching	☐ Repetitive Movement	☐ Bending
☐ Eye strain	☐ Machinery (portable)	☐ Hand tools
Other/Details:		
Biological (e.g. hygiene, disease, infection)		
☐ Human tissue/fluids	☐ Virus / Disease	☐ Food handling
☐ Microbiological	☐ Animal tissue/fluids	☐ Allergenic
Other/Details:		
Chemicals Note: Refer to the label and Safety Data Sheet (SDS) for the classification and management of all chemicals.		
☐ Non-hazardous chemical(s)	☐ 'Hazardous' chemical (Refer to a completed hazardous chemical risk assessment)	
☐ Engineered nanoparticles	☐ Explosives	☐ Gas Cylinders
Name of chemical(s) / Details:		
Critical Incident – resulting in:		
☐ Lockdown	☐ Evacuation	☐ Disruption
☐ Public Image/Adverse Media Issue	☐ Violence	☐ Environmental Issue
Other/Details:		
Radiation		
☐ Ionising radiation	☐ Ultraviolet (UV) radiation	☐ Radio frequency/microwave
☐ infrared (IR) radiation	☐ Laser (class 2 or above)	☐
Other/Details:		
Energy Systems – incident / issues involving:		
☐ Electricity (incl. Mains and Solar)	☐ LPG Gas	☐ Gas / Pressurised containers
Other/Details:		
Facilities / Built Environment		
☐ Buildings and fixtures	☐ Driveway / Paths	☐ Workshops / Work rooms
☐ Playground equipment	☐ Furniture	☐ Swimming pool
Other/Details:		
People issues		
☐ Students	☐ Staff	☐ Visitors / Others
☒ Physical	☐ Psychological / Stress	☐ Contractors
☐ Fatigue	☐ Workload	☐ Organisational Change
☐ Workplace Violence/Bullying	☐ Inexperienced/new personnel	☐
Other/Details: Physical - Dropping equipment on feet etc..		

Step 1 (cont) Other Hazards / Details(enter other hazards not identified on the table)
Damage to eyes - Exposure to laser radiation (Class 1). Hazard is minimal with class 1 laser. Risk is low if fully enclosed.
Irritation to skin/eyes - Exposure to fibre glass shards/dust
Hearing Damage - Exposure to sound up to 92dB for periods longer than an hour

Risk Matrix

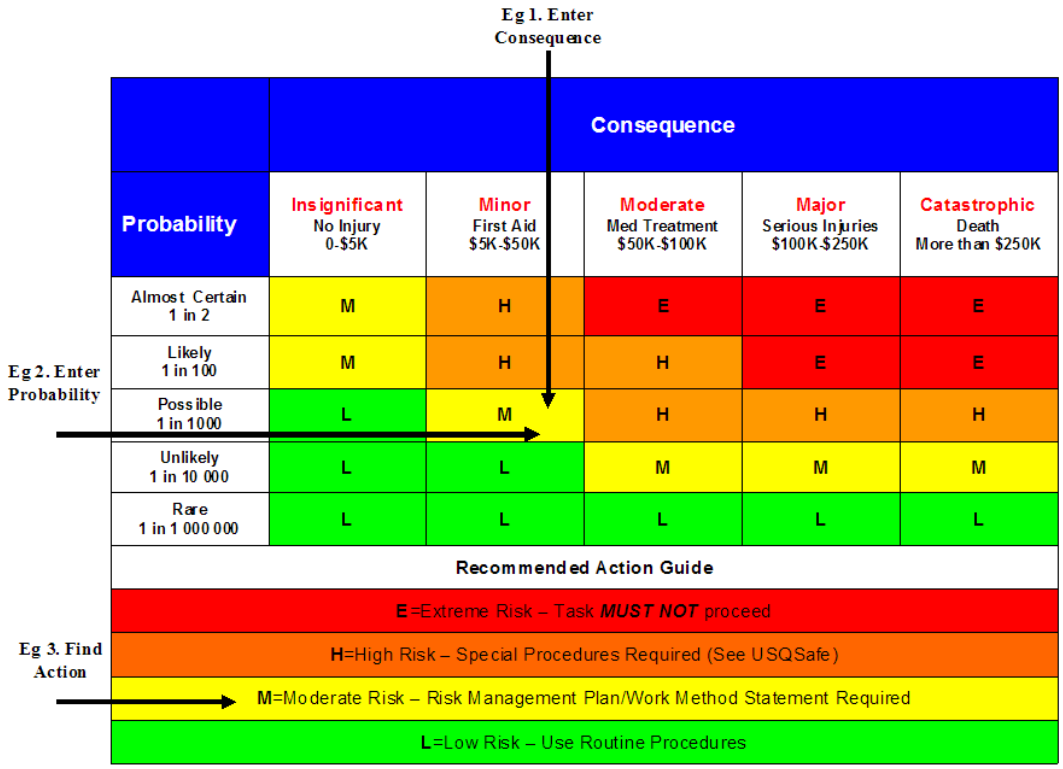

Risk register and Analysis

Step 1 (cont)	Step 2	Step 2a	Step 3			Step 4				
Hazards: From step 1 or more if identified	**The Risk:** What can happen if exposed to the hazard with existing controls in place?	**Existing Controls:** What are the existing controls that are already in place?	**Risk Assessment:** (use the Risk Matrix on p3) Consequence x Probability = Risk Level			**Additional controls:** Enter additional controls if required to reduce the risk level	**Risk assessment with additional controls:** (use the Risk Matrix on p3 – has the consequence or probability changed?)			**Controls Implemented? Yes/No**
			Consequence	**Probability**	**Risk Level**		**Consequence**	**Probability**	**Risk Level**	
Example										
Working in temperatures over 35^0 C	Heat stress/heat stroke/exhaustion leading to serious personal injury/death	Regular breaks, chilled water available, loose clothing, fatigue management policy.	catastrophic	possible	Mod	temporary shade shelters, essential tasks only, close supervision, buddy system	catastrophic	unlikely	Low	Yes
Setting up, taking down and inspecting equipment	Personal Injury Electric Shock Damage to equipment	Wearing enclosed footwear Compliant and properly earthed equipment Earth leakage protection	Moderate	Rare	Low	Ensure equipment is disconnected from power supply while being set up, taken down or inspected. Care must be taken in moving equipment that it is not dropped or bumped. Optical fibre should not be bent beyond the bend radius	Moderate	Rare	Low	Yes
Energising equipment	Electric Shock Damage to equipment Eye damage	Compliant and properly earthed equipment Earth leakage protection Safe working procedures	Moderate	Rare	Low	Optical outputs must be connected before system is energised and remain connected until it is de-energised. Optical source light must be fully enclosed in optical fibre Laser safety glasses appropriate for the wavelength in use must be worn	Moderate	Rare	Low	Yes
De-Energising Equipment	Eye damage Electric Shock	Safety glasses	Moderate	Rare	Low	PPE must be worn until system is completely de-energised	Moderate	Rare	Low	Yes
Mechanical Splice	Damage or irritation to skin and eyes	Safe working procedures as per Thorlabs FN96A http://www.thorlabs.hk/thorcat/1100/FN96A-Manual.pdf	Moderate	Rare	Low	Care must be taken in using tools PPE - Safety glasses	Moderate	Rare	Low	Yes
Filing/Polishing fibre	Damage or irritation to skin and eyes	Safety Glasses must be worn Latex gloves must be worn	Select a consequence	Select a probability	Select a Risk Level	Care must be taken when polishing/filing fibre that no shards or dust get on skin or eyes	Moderate	Rare	Low	Yes

Step 1 (cont)	Step 2	Step 2a	Step 3			Step 4				
Hazards: From step 1 or more if identified	**The Risk:** What can happen if exposed to the hazard with existing controls in place?	**Existing Controls:** What are the existing controls that are already in place?	**Risk Assessment:** (use the Risk Matrix on p3) Consequence x Probability = Risk Level			**Additional controls:** Enter additional controls if required to reduce the risk level	**Risk assessment with additional controls:** (use the Risk Matrix on p3 – has the consequence or probability changed?)			Controls Implemented? Yes/No
			Consequence	Probability	Risk Level		Consequence	Probability	Risk Level	
Example										
Working in temperatures over 35^{0} C	Heat stress/heat stroke/exhaustion leading to serious personal injury/death	Regular breaks, chilled water available, loose clothing, fatigue management policy.	catastrophic	possible	Mod	temporary shade shelters, essential tasks only, close supervision, buddy system	catastrophic	unlikely	Low	Yes
Producing tones during testing	Hearing Damage	PPE - Hearing Protection	Moderate	Rare	Low	Ensure tones are produced only as long as neccesary for testing	Moderate	Rare	Low	Yes or No
			Select a consequence	Select a probability	Select a Risk Level		Select a consequence	Select a probability	Select a Risk Level	Yes or No
			Select a consequence	Select a probability	Select a Risk Level		Select a consequence	Select a probability	Select a Risk Level	Yes or No
			Select a consequence	Select a probability	Select a Risk Level		Select a consequence	Select a probability	Select a Risk Level	Yes or No
			Select a consequence	Select a probability	Select a Risk Level		Select a consequence	Select a probability	Select a Risk Level	Yes or No
			Select a consequence	Select a probability	Select a Risk Level		Select a consequence	Select a probability	Select a Risk Level	Yes or No
			Select a consequence	Select a probability	Select a Risk Level		Select a consequence	Select a probability	Select a Risk Level	Yes or No
			Select a consequence	Select a probability	Select a Risk Level		Select a consequence	Select a probability	Select a Risk Level	Yes or No
			Select a consequence	Select a probability	Select a Risk Level		Select a consequence	Select a probability	Select a Risk Level	Yes or No
			Select a consequence	Select a probability	Select a Risk Level		Select a consequence	Select a probability	Select a Risk Level	Yes or No
			Select a consequence	Select a probability	Select a Risk Level		Select a consequence	Select a probability	Select a Risk Level	Yes or No
			Select a consequence	Select a probability	Select a Risk Level		Select a consequence	Select a probability	Select a Risk Level	Yes or No
			Select a consequence	Select a probability	Select a Risk Level		Select a consequence	Select a probability	Select a Risk Level	Yes or No
			Select a consequence	Select a probability	Select a Risk Level		Select a consequence	Select a probability	Select a Risk Level	Yes or No
			Select a consequence	Select a probability	Select a Risk Level		Select a consequence	Select a probability	Select a Risk Level	Yes or No
			Select a consequence	Select a probability	Select a Risk Level		Select a consequence	Select a probability	Select a Risk Level	Yes or No
			Select a consequence	Select a probability	Select a Risk Level		Select a consequence	Select a probability	Select a Risk Level	Yes or No
			Select a consequence	Select a probability	Select a Risk Level		Select a consequence	Select a probability	Select a Risk Level	Yes or No
			Select a consequence	Select a probability	Select a Risk Level		Select a consequence	Select a probability	Select a Risk Level	Yes or No

Step 1 (cont)	Step 2	Step 2a	Step 3			Step 4				
Hazards: From step 1 or more if identified	**The Risk:** What can happen if exposed to the hazard with existing controls in place?	**Existing Controls:** What are the existing controls that are already in place?	**Risk Assessment:** (use the Risk Matrix on p3) Consequence x Probability = Risk Level			**Additional controls:** Enter additional controls if required to reduce the risk level	**Risk assessment with additional controls:** (use the Risk Matrix on p3 – has the consequence or probability changed?)			**Controls Implemented? Yes/No**
			Consequence	**Probability**	**Risk Level**		**Consequence**	**Probability**	**Risk Level**	
Example										
Working in temperatures over 35^0 C	Heat stress/heat stroke/exhaustion leading to serious personal injury/death	Regular breaks, chilled water available, loose clothing, fatigue management policy.	catastrophic	possible	Mod	temporary shade shelters, essential tasks only, close supervision, buddy system	catastrophic	unlikely	Low	Yes
			Select a consequence	Select a probability	Select a Risk Level		Select a consequence	Select a probability	Select a Risk Level	Yes or No
			Select a consequence	Select a probability	Select a Risk Level		Select a consequence	Select a probability	Select a Risk Level	Yes or No

Step5 – Action Plan (for controls not already in place)			
Control Option	**Resources**	**Person(s) responsible**	**Proposed implementation date**
PPE	**Safety Glasses** **Latex Gloves** **Hearing Protection**	**User**	
Do not energise system while seting up, taking down or inspecting equipment		**User**	
Ensure all optical outlets connected before energising		**User**	

Step 6 – Approval

Drafter's Comments:

Drafter Details:

Name: Signature: Date: / /

Assessment Approval:(Extreme or High = VC, Moderate = Cat 4 delegate or above, Low = Manager/Supervisor)

I am satisfied that the risks are as low as reasonably practicable and that the resources required will be provided.

Name: Signature: Date: / /

Position Title:

Appendix C

Laser On/Off Procedures

Laser Procedures

Laser on Procedure

1. Ensure door to the room is unlocked
2. Check optical system is properly connected
3. Check settings on optical source and detector
4. Power up laser equipment (source and detector)
5. Reset emergency stop button and insert the keys (Optical Source)
6. Enable laser

Laser off Procedure

1. Turn laser (source) off
2. Turn off other laser equipment (detector)
3. Remove keys (source)
4. Press in the emergency stop button
5. Remove power supply to laser equipment (source and detector)
6. Remove and store laser safety glasses
7. Turn of external warning sign

Appendix D

Project Time Line

Fibre-optic Microphone Project Timeline

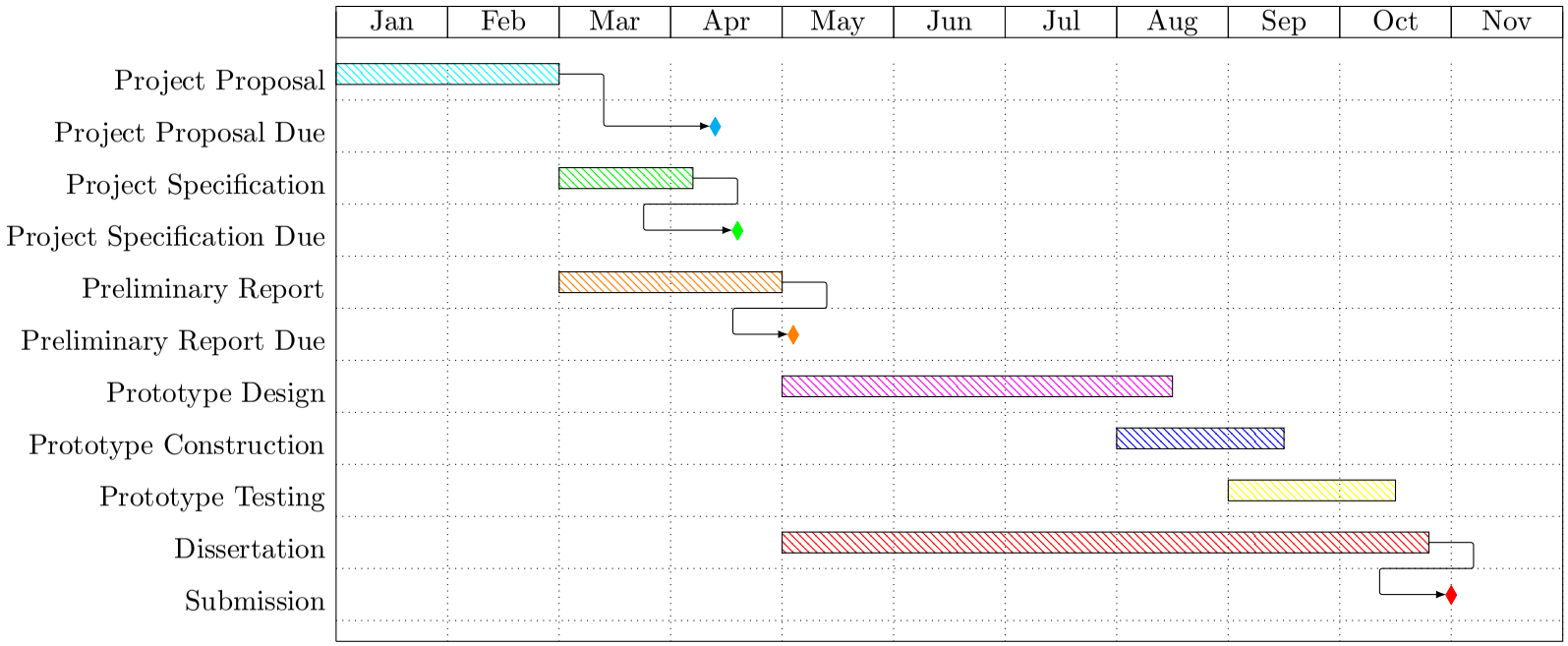

Appendix E

MATLAB Code - Initial Testing Results

```
%% Header
%Initial_Testing.m
%Fibre-Optic Microphone Inital Testing Results
%Author: Isaac Kennedy u1016605
%Created: 8/10/2014
%Last Edited: 27/10/2014

%% clean up workspace
clear all
close all
clc

%% Input
%Recorded Test Results
x = [0:2:16];
T = [0,3.33,20,16.67,33.33,80,86.67,100,156.67];

%Line of best fit - Exponential
f = fit(x',T','exp1');

%% Output
%Plot test results and line of best fit.
figure(1)
hold on
```

```
grid on
h = plot(f,'r-',x,T,'bo');
set(h, 'LineWidth',2)
title('Initial Test 1kHz Response')
xlabel('Speaker Input (V)')
ylabel('Average Response ( \muV)')
hleg1 = legend('Recorded Response','Line of Best Fit');
set(hleg1, 'location', 'northwest')
```

Appendix F

MATLAB Code - Frequency Testing Results

```
%% Header
%Frequency_Testing.m
%Fibre–Optic Microphone Inital Testing Results
%Author: Isaac Kennedy u1016605
%Created: 8/10/2014
%Last Edited: 27/10/2014

%% clean up workspace
clear all
close all
clc

%% Input
%Recorded Test Results – Uncomment relevant section to plot results
%500 Hz
%tit='500Hz Average Response';
%x = [63.57,68.73,73.50,76.33,78.60,80.30,82.17,83.27,84.50];
%T = [0,33.33,33.33,83.33,96.67,120.00,156.67,121.33,280];
%1kHz
%tit='1kHz Average Response';
%x = [64.9,74.33,80.43,83.70,86.17,88,89.73,91.07,92.23];
%T = [0,20,30,53.33,73.33,80,113.33,150,193.33];
%2.5kHz
%tit='2.5kHz Average Response';
```

```
%x =[64.97,70.03,74.83,78.07,80.23,82.33,83.77,85.17,86.60];
%T = [0,3.33,3.33,16.67,16.67,23.33,26.67,36.67,46.67];
%5kHz
%tit='5kHz Average Response';
%x =[64.83,69.13,73.47,77.6,79.43,82.37,86.40,87.77,89.17];
%T = [0,13.33,13.33,26.67,60,80,126.67,136.67,190];
%10kHz
%tit='10kHz Average Microphone Response';
%x = [64.2,69.93,74.53,78.10,80.80,83,85.17,86.43,87.67];
%T = [0,20,26.67,46.67,63.33,70,153.33,160,200];
%15kHz
%tit='15kHz Average Response';
%x =[65.37,72.87,77.73,81.27,83.70,86.03,87.17,88.53,89.87];
%T = [0,16.67,33.33,60,80,100,190,213.33,256.67];
%20kHz
tit='20kHz Average Response';
x =[64.5,66.10,69.33,70.87,74.33,75.53,77.17,78.20,79.03];
T = [0,20,33.33,56.67,110,123.33,133.33,146.67,200];

%% Calculations
%Line of best fit – Exponential
f = fit(x',T','exp1');

%% Output
%Plot test results and line of best fit
figure(1)
hold on
grid on
h = plot(f,'r–',x,T,'bo');
set(h, 'LineWidth',2)
title(tit)
xlabel('Volume Level (dB)')
ylabel('Average Response ( \muV)')
hleg1 = legend('Recorded Response','Line of Best Fit');
set(hleg1, 'location', 'northwest')
```

Appendix G

MATLAB Code - Frequency Testing Comparison

```
%% Header
%Frequency_Comparison.m
%Fibre-Optic Microphone Inital Testing Results
%Author: Isaac Kennedy u1016605
%Created: 8/10/2014
%Last Edited: 27/10/2014

%% clean up workspace
clear all
close all
clc

%% Input
%Recorded Test Results
%500Hz
x1 = [63.57,68.73,73.50,76.33,78.60,80.30,82.17,83.27,84.50];
T1 = [0,33.33,33.33,83.33,96.67,120.00,156.67,121.33,280];

%1kHz
x2 = [64.9,74.33,80.43,83.70,86.17,88,89.73,91.07,92.23];
T2 = [0,20,30,53.33,73.33,80,113.33,150,193.33];

%2.5kHz
x3 =[64.97,70.03,74.83,78.07,80.23,82.33,83.77,85.17,86.60];
```

```
T3 = [0,3.33,3.33,16.67,16.67,23.33,26.67,36.67,46.67];

%5kHz
x4 =[64.83,69.13,73.47,77.6,79.43,82.37,86.40,87.77,89.17];
T4 = [0,13.33,13.33,26.67,60,80,126.67,136.67,190];

%10kHz
x5 = [64.2,69.93,74.53,78.10,80.80,83,85.17,86.43,87.67];
T5 = [0,20,26.67,46.67,63.33,70,153.33,160,200];

%15kHz
x6 =[65.37,72.87,77.73,81.27,83.70,86.03,87.17,88.53,89.87];
T6 = [0,16.67,33.33,60,80,100,190,213.33,256.67];

%20kHz
x7 =[64.5,66.10,69.33,70.87,74.33,75.53,77.17,78.20,79.03];
T7 = [0,20,33.33,56.67,110,123.33,133.33,146.67,200];

%% Calculations
%Line of best fit – Exponential

%500Hz
f1 = fit(x1',T1','exp1');
c1 = coeffvalues(f1);
b1 = c1(1);
m1 = c1(2);
xexp1 = [min(x1):0.1:max(x1)];
exp1 = b1*exp(m1*xexp1);

%1kHz
f2 = fit(x2',T2','exp1');
c2 = coeffvalues(f2);
b2 = c2(1);
m2 = c2(2);
xexp2 = [min(x2):0.1:max(x2)];
exp2 = b2*exp(m2*xexp2);

%2.5kHz
f3 = fit(x3',T3','exp1');
c3 = coeffvalues(f3);
b3 = c3(1);
m3 = c3(2);
xexp3 = [min(x3):0.1:max(x3)];
```

```
exp3 = b3*exp(m3*xexp3);

%5kHz
f4 = fit(x4',T4','exp1');
c4 = coeffvalues(f4);
b4 = c4(1);
m4 = c4(2);
xexp4 = [min(x4):0.1:max(x4)];
exp4 = b4*exp(m4*xexp4);

%10kHz
f5 = fit(x5',T5','exp1');
c5 = coeffvalues(f5);
b5 = c5(1);
m5 = c5(2);
xexp5 = [min(x5):0.1:max(x5)];
exp5 = b5*exp(m5*xexp5);

%15kHz
f6 = fit(x6',T6','exp1');
c6 = coeffvalues(f6);
b6 = c6(1);
m6 = c6(2);
xexp6 = [min(x6):0.1:max(x6)];
exp6 = b6*exp(m6*xexp6);

%20kHz
f7 = fit(x7',T7','exp1');
c7 = coeffvalues(f7);
b7 = c7(1);
m7 = c7(2);
xexp7 = [min(x7):0.1:max(x7)];
exp7 = b7*exp(m7*xexp7);

%% Output
%Plot all results of frequency testing on a single plot including data
%points and line of best fit.

tit = 'Frequency Response Comparison';
figure(1)
hold on
grid on
plot(xexp1,exp1,xexp2,exp2,xexp3,exp3,xexp4,exp4,xexp5,exp5,xexp6,exp6,xexp7,exp7,'LineWidth',2
```

```
plot(x1,T1,'o',x2,T2,'o',x3,T3,'o',x4,T4,'o',x5,T5,'o',x6,T6,'o',x7,T7,'o','LineWidth',2)
axis([60 95 −20 300])
title(tit)
xlabel('Volume (dB)')
ylabel('Average Response ( \muV)')
hleg1 = legend('500Hz','1kHz','2.5kHz','5kHz','10kHz','15kHz','20kHz');
set(hleg1, 'location', 'northwest')
```

Appendix H

MATLAB Code - Laser Power Level Testing Results

```
%% Header
%Power_Comparison.m
%Fibre-Optic Microphone Inital Testing Results
%Author: Isaac Kennedy u1016605
%Created: 8/10/2014
%Last Edited: 27/10/2014

%% clean up workspace
clear all
close all
clc

%% Input
%Recorded Test Results

%0.05mW
x1=[59.9,71.2,76.1,78.8,81.5,83.2,84.7,86.1,87.4];
p1=[0,0,0,0,0,0,0,0,0];

%0.1mW
x2=[65.1,70.6,75.3,78.4,81.5,83.8,85.5,86.5,87.1];
p2=[0,0,0,0,0,0,10,10,20];

%0.2mW
```

```
x3=[65.1,70.9,76.3,79.8,82.2,84.1,85.2,86.7,87.7];
p3=[0,0,10,20,10,50,50,50,50];

%0.3mW
x4=[65.1,70.9,76.3,79.8,82.2,84.1,85.2,86.7,87.7];
p4=[0,0,0,20,20,60,60,60,70];



%0.5mW
x5=[65.2,71.3,76.5,79.5,82.1,83.9,85.5,86.7,87.7];
p5=[0,20,40,30,70,90,170,150,210];

%0.7mW
x6=[65,71.3,76.5,79.6,81.7,83.9,85.5,86.8,88.1];
p6=[0,20,30,120,80,150,200,260,290];

%0.9mW
x7=[65.2,70.6,75.9,78.9,81.5,83.3,84.9,86.2,87.3];
p7=[0,20,20,130,150,160,320,400,450];

%% Calculations
%Line of best fit – Exponential

%500Hz
f1 = fit(x1',p1','exp1');
c1 = coeffvalues(f1);
b1 = c1(1);
m1 = c1(2);
xexp1 = [min(x1):0.1:max(x1)];
exp1 = b1*exp(m1*xexp1);

%1kHz
f2 = fit(x2',p2','exp1');
c2 = coeffvalues(f2);
b2 = c2(1);
m2 = c2(2);
xexp2 = [min(x2):0.1:max(x2)];
exp2 = b2*exp(m2*xexp2);

%2.5kHz
f3 = fit(x3',p3','exp1');
c3 = coeffvalues(f3);
b3 = c3(1);
```

```
m3 = c3(2);
xexp3 = [min(x3):0.1:max(x3)];
exp3 = b3*exp(m3*xexp3);

%5kHz
f4 = fit(x4',p4','exp1');
c4 = coeffvalues(f4);
b4 = c4(1);
m4 = c4(2);
xexp4 = [min(x4):0.1:max(x4)];
exp4 = b4*exp(m4*xexp4);

%10kHz
f5 = fit(x5',p5','exp1');
c5 = coeffvalues(f5);
b5 = c5(1);
m5 = c5(2);
xexp5 = [min(x5):0.1:max(x5)];
exp5 = b5*exp(m5*xexp5);

%15kHz
f6 = fit(x6',p6','exp1');
c6 = coeffvalues(f6);
b6 = c6(1);
m6 = c6(2);
xexp6 = [min(x6):0.1:max(x6)];
exp6 = b6*exp(m6*xexp6);

%20kHz
f7 = fit(x7',p7','exp1');
c7 = coeffvalues(f7);
b7 = c7(1);
m7 = c7(2);
xexp7 = [min(x7):0.1:max(x7)];
exp7 = b7*exp(m7*xexp7);

%% Output
%Plot all results of power testing on a single plot including data
%points and line of best fit.


tit= 'Laser Power Level Comparison';
figure(1)
```

```
hold on
grid on
plot(xexp1,exp1,xexp2,exp2,xexp3,exp3,xexp4,exp4,xexp5,exp5,xexp6,exp6,xexp7,exp7,'LineWidth',2
plot(x1,p1,'o',x2,p2,'o',x3,p3,'o',x4,p4,'o',x5,p5,'o',x6,p6,'o',x7,p7,'o','LineWidth',2)
title(tit)
axis([60 90 -20 450])
xlabel('Volume Level (dB)')
ylabel('Measured Response Response (\muV)')
hleg1 = legend('0.05mW','0.1mW','0.2mW','0.3mW','0.5mW','0.7mW','0.9mW');
set(hleg1, 'location', 'northwest')
```